South Dakota State University

Open PRAIRIE: Open Public Research Access Institutional Repository and Information Exchange

Theses and Dissertations

2016

Soil Salinity Study in Northern Great Plains Sodium Affected Soil

Tulsi P. Kharel

South Dakota State University

SOIL SALINITY STUDY IN NORTHERN GREAT PLAINS SODIUM AFFECTED SOIL

BY

TULSI P KHAREL

A dissertation submitted in partial fulfillment of the requirements for the

Doctor of Philosophy

Major in Plant Science

South Dakota State University

2016

SOIL SALINITY STUDY IN NORTHERN GREAT PLAINS SODIUM AFFECTED SOIL

This dissertation is approved as a creditable and independent investigation by a candidate for the Doctor of Philosophy degree and is acceptable for meeting the dissertation requirements for this degree. Acceptance of this dissertation does not imply that the conclusions reached by the candidate are necessarily the conclusions of the major department.

5/20/2016

David E. Clay, Ph. D. Date

Dissertation Advisor

5.20.2016

David Wright, Ph. D. Date

Head, Plant Science Department

24 May 2016

Dean, Graduate School Date

ACKNOWLEDGEMENTS

I would like to thank my committee members: Dr. David Clay, Dr. Sharon Clay, Dr. Douglas Malo, Dr. Gregg Carlson, Dr. Cheryl Reese, Dr. Gary Hatfield and Dr. Adam Hoppe. Their input as committee members from the beginning of this research design and development to data analysis shaped this dissertation with the outcomes presented. Several months of data to information extraction, writing and summarizing these outcomes as a valuable addition to scientific knowledge was another intensive, rigorous learning process from my advisor, Dr. David Clay.

This dissertation would not have been possible without the help of lab members, and co-graduate students working together on this soil salinity project. I would like to thank all of them for their help and contribution for the success of this study.

TABLE OF CONTENTS

ABBREVIATIONS

ANOVA	Analysis of variance
B1-B11	Landsat 5, 7 and 8 Bands
BI	Brightness Index
BMP	Best Management Practices
Br	Bromide
Ca	Calcium
$CaCl_2$	Calcium Chloride
CART	Classification and Regression Tree
CEC	Cation Exchange Capacity
CI	Confidence Interval
cm	Centimeter
$cmol_c$	Centimol charge
dEC	Change in EC
DEM	Digital Elevation Model
DGPS	Differentially Corrected Global Positioning System
dNa	Change in Na
dS	DesiSeimen
dSAR	Change in SAR
EC	Electrical Conductivity
ESP	Exchangeable Sodium Percentage
ETM+	Enhanced Thematic Mapper Plus
EVI	Enhanced Vegetation Index
GridMet	Gridded Surface Meteorological
gSSURGO	Gridded Soil Survey Geographic
H_2SO_4	Sulfuric Acid
ha	Hectares
hr	Hour
KBr	Potassium Bromide

LCC	Land Capability Class
LiDAR	Light Detection and Ranging
LOESS	Locally weighted polynomial regression
LR	Linear Regression
LSD	Least significant difference
M	Molar
Mg	Magnesium
MIRBI	Mid Infrared Burn Index
ml	Milliliter
mm	Millimeter
MODIS	Moderate Resolution Imaging Spectroradiometer
MSE	Mean Square Error
MSR16R	Multispectral Radiometer, Crop Scan unit
Na	Sodium
NASS	National Agricultural Statistics Service
NDMI	Normalized Difference Moisture Index
NDSI	Normalized Difference Salinity Index
NDVI	Normalized Difference Vegetation Index
NDWI	Normalized Difference Water Index
NGP	Northern Great Plains
NIR	Near infrared
NRCS	Natural Resource Conservation Service
OLI/TIRS	Operational Land Imager/Thermal Infrared Sensors
P value	Probability of Significance
PC	Principle Component
ppm	Parts Per Million
Precip.	Precipitation in mm for growing season
PV	Pore Volume
R^2	Coefficient of Determination

RF	Random Forest
RT	Regression Tree
S.D.	Standard Deviation
SAR	Sodium Absorption Ratio
SAVI	Soil Adjusted Vegetation Index
SD	South Dakota
SI	Salinity Index
SSURGO	Soil Survey Geographic
SWIR	Short Wave infrared
Tmax	Maximum Temperature in ^{o}K for growing season
Tmin	Minimum Temperature ^{o}K for growing season
TOA	Top of Atmosphere
USDA	United States Department of Agriculture
VIF	Variance Inflation Ratio
τ	Time series monotonic trend (Mann-Kendall test)

LIST OF TABLES

Chapter 1

Chapter 2

LIST OF FIGURES

Chapter 1

Chapter 2

PROBLEM STATEMENT

Increasing temperature and precipitation are the major contributors for the expanding saline and sodic areas in the Northern Great Plains. Climate and land-use changes combined with Northern Great Plains high sodium parent materials have increased both salinization and sodification risks. Techniques and methods are needed to track and manage this growing problem. Objectives of this research study were to 1) compare three chemical amendments (calcium chloride, sulfuric acid and gypsum) with water to determine the remediation strategies on water permeability and Na transport in undisturbed soil columns and 2) to develop a remote-sensing model that can be used to identify the extent of soil salinization problem.

ABSTRACT

SOIL SALINITY STUDY IN NORTHERN GREAT PLAINS SODIUM AFFECTED SOIL

TULSI P KHAREL

2016

Climate and land-use changes when combined with the marine sediments that underlay portions of the Northern Great Plains have increased the salinization and sodification risks. The objectives of this dissertation were to compare three chemical amendments (calcium chloride, sulfuric acid and gypsum) remediation strategies on water permeability and sodium (Na) transport in undisturbed soil columns and to develop a remote sensing technique to characterize salinization in South Dakota soils. Forty-eight undisturbed soil columns (30 cm x 15 cm) collected from White Lake, Redfield, and Pierpont were used to assess the chemical remediation strategies. In this study the experimental design was a completely randomized design and each treatment was replicated four times. Following the application of chemical remediation strategies, 45.2 cm of water was leached through these columns. The leachate was separated into 120-ml increments and analyzed for Na and electrical conductivity (EC). Sulfuric acid increased Na leaching, whereas gypsum and $CaCl_2$ increased water permeability. Our results further indicate that to maintain effective water permeability, ratio between soil EC and sodium absorption ratio (SAR) should be considered.

In the second study, soil samples from 0-15 cm depth in 62 x 62 m grid spacing were taken from the South Dakota Pierpont (65 ha) and Redfield (17 ha) sites. Saturated paste EC was measured on each soil sample. At each sampling points reflectance and derived indices (Landsat 5, 7, 8 images), elevation, slope and aspect (LiDAR) were extracted. Regression models based on multiple linear regression, classification and regression tree, cubist, and random forest techniques were developed and their ability to predict soil EC were compared. Results showed that: 1) Random forest method was found to be the most effective method because of its ability to capture spatially correlated variation, 2) the short wave infrared (1.5 -2.29 µm) and near infrared (0.75-0.90 µm) were very sensitive to soil salinity; 3) EC prediction model using all 3 season (spring, summer and fall) images was better on state wide validation dataset compared to individual season model. Finally, in eastern South Dakota, the model predicted that from 2008 to 2012, EC increased in 569,165 ha or 13.4% of the land seeded to corn (*Zea mays L.*) or soybeans (*Glycine max L*).

Chapter 1

Developing criteria for identifying high risk saline/sodic soils

Summary

Climate and land-use changes combined with Northern Great Plains high sodium parent materials have increased the salinization and sodification risks. The objectives in this study were to assess the effectiveness of chemical remediation on improving soil health and to determine benchmarks for identifying high risk saline/sodic soils. Forty eight soil columns (16 per site) collected from three sites of South Dakota (White Lake, Redfield and Pierpont) were used for this purpose. The undisturbed soil columns were treated one of four treatment (none, $CaCl_2$, gypsum, and sulfuric acid). To track water movement all columns were treated with KBr. The movement of Na, Br, and other salts through the soil was quantified. At the beginning of the study all columns were characterized as saline/sodic. A completely randomized design was used with four treatments and four replications. 45.2 cm of water was leached through these columns. The leachate was collected in 120-ml increments, which were analyzed for Na, Br, and EC. The permeability of the soil was calculated and soil columns were dissected and analyzed for Br, Na, Ca, and Mg. At the initiation of the experiment, all columns demonstrated by-pass flow. The amount of by-pass flow decreased with increasing EC to SAR ratio. The H_2SO_4 treatment increased Na leaching, whereas gypsum and $CaCl_2$ increased water permeability. These findings were attributed to gypsum and $CaCl_2$ providing a Ca source that helped rebuild the soil structure. Our result further indicated that to maintain effective water permeability, soil EC to SAR ratio should be >1.

Introduction

Climatic records indicate that spring temperatures and rainfall have increased in the Northern Great Plains (NGP) (Hatfield et al., 2011; Schrag, 2011; Kunkel et al., 2013; Shafer et al., 2014), and these changes, when combined with improved genetics, crop insurance, and better equipment contributed to the conversion of 728,000 ha of South Dakota grassland to cropland between 2006 and 2012 (Reistma et al., 2015), and the conversion of 216,000 ha of North Dakota grasslands to cropland between 2007 and 2008 (McCombie, 2009). Climate and land-use changes when combined with high sodium concentrations in one of the region's parent material (marine sediments) have increased the salinization and sodification risks. The regions marine sediments contain high concentrations of both Na and other salts. Worldwide, salinization and sodification are often linked to irrigation, whereas in South Dakota and North Dakota the expanding problem is associated with increased spring precipitation, and warmer temperatures. In soils derived over marine sediments, a rising water table provides an opportunity to transport subsurface salts to the soil surface through capillary action (Rhoades and Halverson, 1976; Seelig, 2000, Carlson et al., 2016).

In the NGP, it is estimated that 10.6 million hectares of Minnesota (20,100 ha), Montana (4,380,000 ha), Nebraska (56,800 ha), North Dakota (2,350,000 ha), South Dakota (3,442,000 ha) and Wyoming (445,344 ha) land are impacted by saline conditions (Seelig, 2000; Millar, 2003; Hopkins et al., 2012; Carlson et al., 2013; Soil Survey Staff), and over 2 million hectares of land are impacted by high Na concentration in South Dakota (1,200,000 ha) and North Dakota (800,000 ha) (Millar, 2003; Seelig, 2000). In these soils, the common Na containing salts are sodium sulfate (Na_2SO_4) and sodium carbonate (Na_2CO_3). High Na minerals can also result in high soil pH which can reduce the availability of some nutrients (N, P, Fe, Mn, Cu, and Zn). In a saline soil that contains free lime ($CaCO_3$), the maximum pH is approximately 8.4, whereas in sodic soils that contains Na_2CO_3, the pH can increase above this value.

The impacts of saline-affected soils on food security and the economic viability of rural communities has been staggering. For example, due to high salt concentrations [EC$\geq$ 4 dS/m] there is an annual economic loss of $26.2 million/year on 113,000 ha of land located in the South Dakota counties of Beadle, Brown, and Spink (NRCS, 2012), and a loss of $150 million in North Dakota's Red River Valley (Hadrich, 2012). With over 10.6 million ha of saline soils in the NGP in a vulnerable position and many more worldwide quicker assessing techniques and effective management strategies are needed.

Historically, salt classification of soils has been based on EC using the saturated paste method and Sodium Absorption Ratio (SAR). Based on these values, the soil is classified as normal (EC<4dS/m and SAR <13 $mmol_c\,L^{-0.5}$), saline (EC>4dS/m and SAR < 13 $mmol_c\,L^{-0.5}$), saline-sodic (EC>4 dS/m and SAR>13 $mmol_c\,L^{-0.5}$) or sodic (EC<4dS/m and SAR>13 $mmol_c\,L^{-0.5}$). The traditional remediation strategy of installing tile drainage and leaching with high quality water can result in serious problems in the NGP. Draining these sites, may accelerate the problems. Recommended solutions to the problem include applying a chemical treatment such as gypsum, calcium chloride, or elemental S, followed by planting salt tolerant plants, such as kochia (*Kochia scorparia*) and foxtail barley (*Hordeum jubatum*) (Custer, 1976). Following drainage, farmers in this region have observed elevated yields for few years. However, high yields do not last, and can be followed by soil dispersion if the Na concentrations are high.

In sodic soils, the addition of gypsum (or some other soluble calcium amendments) can increase the potential for Na to leach. However, if the sodium-affected soil also contains high salts, adding gypsum may increase iron deficiency chlorosis in soybeans (Franzen and Richardson, 2000). In addition, if the soil is saturated with gypsum, the application of gypsum will have minimal impact on soil remediation. The objectives in this study were to assess the effectiveness of chemical remediation on improving soil health and to determine benchmarks for identifying high risk saline/sodic soils

Materials and Methods

Study site

The experiment was designed to mimic the instillation of tile drainage in the regions saline and saline/sodic soils. In the Northern Great Plains, EC of rain water is low and generally < 0.015 dS/m (http://nadp.sws.uiuc.edu/nadpdata/register.asp). Throughout semi-arid glaciated regions, there are landscapes and soils that are characterized as having high concentrations of sodium as well as other salts. The regions saline/sodic soils are generally found in poorly drained footslope areas, and they are often devoid of vegetation.

Collecting soil columns

Forty-eight undisturbed soil columns with the dimensions of 30 cm length by 15 cm diameter were collected between 2011 and 2012 from 3 South Dakota sites (White Lake, 43°40’32’’ N and 98°45’50’’ W; Redfield, 44°58’10’’N and 98°27’45’’W; Pierpont, 45°30’35’’ N, 97°53’47’’W). Soil at White Lake was fine montmorrilonitic, messic typic aguistolls. Soil at Redfield site was fine, smectitic, frigid, pachic argiudolls. Soil at Pierpont site was fine, smectitic calcic natrudolls. For baseline soil properties, soil samples (0- to 15- and 15- to 30- cm) collected adjacent to the column were air-dried (40° C), ground, and sieved through 2 mm screen. Approximately, 150 ml of Type I (high purity deionized nanopure) water was added to 250 g of ground samples to make a saturated paste. Saturated paste extracts were analyzed for soil pH (USSL, Handbook 60, 1954), EC (dS/m) (Whitney, 2015), Na (ppm), Ca (ppm) and Mg (ppm) (Warncke and Brown, 2015) concentrations. Soil pH and EC were measured with accumet Excell XL60 (Fisher Scientific) instruments, while Na, Ca and Mg were measured with an Atomic Absorption spectrometer, model 200A (Buck Scientific). SAR values were calculated after converting Na, Ca and Mg readings to $mmol_c\ L^{-1}$. The SAR values were converted to exchangeable sodium percentage (ESP) using Oster and Sposito (1980).

Table 1.1 Range of values for initial chemical properties of surface 15 cm soil.

Study	Saturated Paste									
	pH	EC	SAR	Na	Ca	Mg	ESP	CEC	N	C
		dS/m		µg/ml	µg/ml	µg/ml	%	cmolc/kg	g/kg	g/kg
White lake	8-8.4	7.7-17.7	2.8-20.5	351-3437	369-694	538-1628	2.8-22.5	44	2.3	23.5
Redfield	8-8.8	3.2-9.9	1.7-6.2	176-1036	216-508	157-1046	1.3-7.3	41	2.3	24.8
Pierpont	7.5-8.4	1.8-22.3	2.2-20.2	151-5032	259-1902	68 -2590	1.9-22.2	39	1.6	18.0

Table 1.2 Chemical treatments applied to columns.

Study	Treatments		
	Gypsum	$CaCl_2$	H_2SO_4
	kg/ha	kg/ha	kg/ha
White lake	5050	4300	930
Redfield	1483	1432	315
Pierpont	5050	4300	930

Salt treatment calculation

Based on baseline soil ESP values (Table 1.1), the salt treatments for each site were calculated. Soil from White Lake and Pierpont had an average exchangeable sodium percentage of 15%, whereas Redfied soil had a maximum ESP value of 7%. Treatment rate calculated based on these values were identical for White Lake and Pierpont and lower rate for Redfield site. For all sites, the target ESP value was 3%. The calculation for estimating the chemical remediation treatment was based on a cation exchange capacity of 25 $cmol_c\ kg^{-1}$ soil and a bulk density of 1.3 $g\ cm^{-3}$. The amount of reagent grade $CaCl_2$ ($CaCl_2.2H_2O$), H_2SO_4, and gypsum (CaSO4. $2H_2O$) were calculated for the surface 15 cm soil (Carlson et al, 2015) (Table 1.2). Potassium bromide (KBr) was applied at 0.874 g per column (Clay et al, 2004) as a water movement tracer. The soil columns were placed on wooden bench prepared to hold them for the experiment. Acid washed sand (10% hydrochloric acid) was placed at the base of each soil column.

The columns were preconditioned by leaching them with 1 pore volume (PV) of type I (nanopure) water. One PV of water corresponds 14.7 cm of rainfall for White Lake site and 11.3 cm of rainfall for Redfield and Pierpont site. Twenty-four hour after preconditioning, the chemical remediation and KBr treatments were applied to the columns. Each of the salt treatment was prepared with 50 ml of water. Hence, 50 ml of H_2SO_4 (1.05M), 50 ml of $CaCl_2$ dissolved solution and 50 ml of nanopure water was applied uniformly at the top of soil surface as H_2SO_4, $CaCl_2$ and control treatment. For gypsum treatment, reagent grade powder gypsum was applied uniformly at the surface and 50 ml water was added later.

Following the surface treatments, 2 pore volumes of type I water was applied to the columns. The leachate was separated into 120 ml increments, which were analyzed for pH, Br, EC and Na. Following the first leaching, the experiment was repeated 24 hours later. In the second leaching experiment, chemical remediation treatments were not applied. Leachate was collected in 120 ml increments and analyzed for pH, Br, EC and Na.

Total sodium removed from each soil column during entire leaching period was calculated using the equation:

$$\mathrm{Na\ (mg)} = \sum_{\mathrm{i}}^{\mathrm{n}} \frac{\mathrm{Na_{ppm}}}{1000} \times \text{ leachate volume (mL)} \qquad [1]$$

where, i to n was the number of leachate samples, leachate volume was 120 mL, and Na_{ppm} was the concentration of Na in each leachate sample.

At the end of the leaching experiment, the soil samples of the columns from White Lake were separated into the 0-5, 5-10, 10-15 and 15-30 cm depth interval. Soil columns from Redfield and Pierpont were separated into the 0-5, 5-10, 10-15 and 15-23 cm depth intervals. The dried and ground soil samples were analyzed for pH, EC, Na, Ca, and Mg.

Data/Statistical analysis

Analysis of covariance was performed on displaced Na setting initial SAR value as a covariate in the model. Data were analyzed using R-statistical program (R Core Team, 2015). Analysis of variance (ANOVA) was performed after adjusting initial SAR and volume of water leached to a constant value for the treatment comparisons. By-pass water flow was evaluated by comparing Br transport through and remaining in the soil.

The statistical R package “lsmean” was used to determine the treatment impacts on Na movement. For nonlinear permeability data visualization local regression smoothing (LOESS) was used in R. Predicted value from LOESS were used to identify critical SAR and EC value assuming 1 mm hr^{-1} permeability as a critical point.

Finding critical point of EC to SAR ratio

Locally weighted polynomial regression (LOESS) was used to establish relationship between permeability to SAR ratio with EC to SAR ratio. Smooth LOESS function was then used for further calculation. The approach used for this calculation was:

1. Find LOESS predictions which represent permeability to SAR ratio (Y) for each value of EC to SAR ratio (X) in data set,
2. Set the critical permeability to 1 mm/hr and use the LOESS predicted value (Y) to find corresponding SAR value using the equations: $Y = \frac{permeability}{SAR}$; $Y = \frac{1\ mm/hr}{SAR}$; $and\ \ SAR = \frac{1 mm/hr}{Y}$,
3. Insert new SAR value for each X into data set to find corresponding EC value using the equation, $X = \frac{EC}{SAR}$; $EC = X * SAR$, and
4. Define the relationship between new SAR and EC (Fig 1.5) as the critical EC and SAR values for maintaining soil permeability.

A similar procedure was followed to calculate the EC and SAR values required to maintain 2 mm/hr permeability through soil column.

Results and Discussion

Site characteristics

The three sites had slightly different characteristics (Table 1.1). At White Lake (WL), the soil pH of the saturated paste ranged from 8 to 8.4 and the saturated paste EC ranged from 7.7 to 17.7 dS/m. The sodium concentration in the saturated paste ranged from 351 to 3437 ppm. At Redfield, the soil pH of the saturated paste ranged from 8 to 8.8, whereas the EC ranged from 3.2 to 9.9 dS/m. At this site, the sodium concentration ranged from 176 to 1036 ppm, and the calculated SAR value ranged from 1.7 to 6.2 $mmol_c\ L^{-0.5}$. At Pierpont (PP) the soil pH ranged from 7.5 to 8.4 and the EC ranged from 1.8 to 22.3 dS/m. The SAR ranged from 2.2 to 20.2 $mmol_c\ L^{-0.5}$. The sodium concentration ranged from 151 to 5032 ppm. The chemical amendments added to the three soils were slightly different. White Lake and Pierpont had identical treatments, whereas Redfield had much lower rates (Table 1.2) due to different initial soil ESP values.

Leaching experiment

The amount of bromide recovered with 0.5 and 2 PV of leaching water was 40 and 90% of the applied Br (Table 1.3). The rapid transport of Br through the columns indicates that by-pass flow occurred. In by-pass flow, a portion of the soil column is bypassed by the water flowing through the soil. A characteristic of by-pass flow is that the tracer (Br^-) appears to flow faster than the water. Others have used Br to track water flow and by-pass flow. For example, Clay et al. (2004) reported similar results in a non-saline/sodic soil where they found only 18, 40 and 57% Br recovery during 0.25, 0.5 and

0.75 PV leachate collection, respectively. In this experiment, Br^- was measured in the leachate prior to 1 pore volume being collected. If bypass flow did not occur, then Br should not have been collected before 1 pore volume.

Table 1.3 Bromide (%) recovered and Na (mg) leached during leaching process and change in soil salinity parameters (dNa, dEC, dSAR) before and after leaching in soil columns.

Treatment	Bromide recovered			Na Leached			Change in Soil Column		
	0.5 PV	2 PV	4 PV	0.5 PV	2 PV	4 PV	dNa	dEC	dSAR
	----- % -----			-------- mg -------			mg	dS/m	
White Lake									
Gypsum	41	90	97	2736	3767	5111	1818	7.96	8.4
$CaCl_2$	48	95	100	4015	5045	6191	1232	7.31	0.4
H_2SO_4	40	85	94	5157	6186	6910	2101	8.6	1.2
Control	33	92	98	2630	3660	4903	2683	10.78	7.5
P value	NS	NS	NS	***	***	***	NS	NS	NS
LSD				876	931	729			
Redfield									
Gypsum	31	90	97	807	1391	2432	140	2.73	2.5
$CaCl_2$	40	93	100	441	1025	2057	253	3.12	3.2
H_2SO_4	43	92	99	761	1345	2440	305	3.72	3.5
Control	43	90	97	768	1353	2376	239	3.96	2.5
P value	NS	NS	NS	0.06	0.12	0.11	NS	NS	NS
LSD				226					
Pierpont									
Gypsum	53	89	95	3077	4794	6654	1839	10.7	9.5
$CaCl_2$	39	86	94	3271	4988	6962	2965	14.6	14
H_2SO_4	41	89	94	3642	5358	7056	1763	10	11.4
Control	51	92	100	1862	3579	5153	1820	11.5	10
P value	NS	NS	NS	***	***	***	NS	NS	NS
LSD				695	731	717			

Note: ! Total Na corresponds for 177 cm^2 surface area and 30 cm depth (White Lake) and 23 cm depth (Redfield and Pierpont).

*0.874 g KBr (587 mg Br) was applied in each column as water tracer

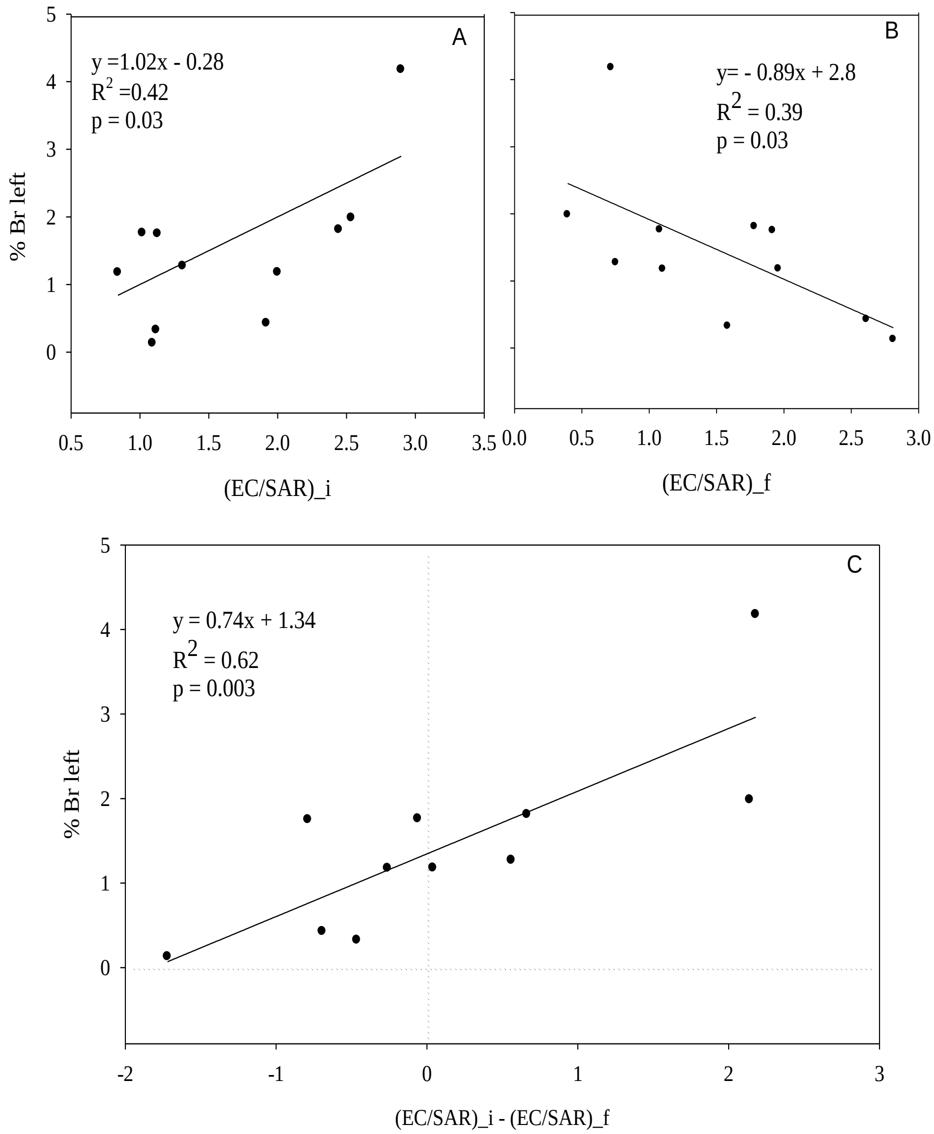

Figure 1.1 Percent Bromide left in control treatment as affected by A) EC to SAR ratio of the soil at the beginning (i=initial), B) EC to SAR ratio of the soil at the end of leaching process (f=final), and C) Difference of EC to SAR ratio between beginning and end samples.

At the end of the leaching study, the % of Br remaining in the soil was related to the soil EC to SAR ratio (Fig.1.1). Given, that the KBr was uniformly applied to the soil surface, it is logical to assume that the amount of Br remaining in the soil at the end of the experiment was related to by-pass flow. Soils with high percentages of Br remaining had high by-pass flow and soils with low amounts of Br remaining had relatively low by-pass flow. The EC to SAR ratio at the beginning of the experiment was directly related to the amount of Br remaining in the surface soil (Fig 1.1A). This interpretation is based on the findings of Flury et al. (1994), who reported that structureless soils had limited by-pass flow, whereas soils with moderate structure had strong by-pass flow characteristics.

The soil EC/SAR ratio at the end of the experiment had an opposite relationship to the amount of remaining Br in the surface soil (Fig 1.1B). To evaluate the cause of this relationship, we compared the amount of Br remaining in the soil vs the change in the EC/SAR ratio (Fig. 1.1C). This comparison suggested that depending on the status of the soils physical conditions, the relative amount of Na lost from the soil changes. In soils with relatively high amounts of Br remaining in the soil, the EC/SAR ratio decreased, whereas in soils with low amounts of Br remaining the opposite was true. These results suggest that sodification was dependent on soil structure. In soils with high levels of Br remaining, the relative amount of Na increased, whereas in soils with low Br remaining, the relative Na concentration decreased.

At all sites and locations, water percolating through the soil removed salts contained in the soil which resulted in decreases in the surface soil EC value (Table 1.3). Others have observed similar findings (Carter and Fanning, 1964; Carter and Robbins, 1978). In columns collected from White Lake 45 cm of water reduced the EC value in the surface 30 cm 74%. Similar decreases were observed for Redfield and Pierpont where EC decreases of 70% were measured in the surface 23 cm. The percent decreases were less than the general rule of leaching proposed by Bresler et al. (1982) where 1 m of water was required to remove 80% of the salt from surface meter of soil. Differences between Bresler at al. (1982) and this study were attributed to by-pass water flow.

Associated with the decrease in the soil EC was a decrease in soluble Na contained in the soil. At White Lake, the amount of soluble Na contained in the soil prior to the study ranged from 3600 mg (or 203 g/ m^2) in the control to 2030 mg (115 g/ m^2) in the $CaCl_2$ treatment. After the study was completed, the amount of soluble Na remaining in the columns ranged from 420 mg (23.73 g/m^2) in the H_2SO_4 to 916 mg (51.75 g/ m^2) in the control. Higher leached sodium in White Lake columns are attributed to a greater amount of water leaching through the soil (6 PV= 88.2 cm). Pierpont and Redfield columns were leached with 4 PV (45.2 cm) of water only. After adjusting the total amount of leached Na to the 4 PV, columns from White Lake and Pierpont had similar results (Table 1.3)

The water by itself contributed to the rapid loss of Na at each site. Compared to the H_2SO_4 treatment, percolating water alone removed 73, 71 and 97% of Na in Pierpont, White Lake and Redfield columns respectively. Several other have reported similar findings (Overstreet et al., 1951; Jury et al., 1979). However, water-based remediation can be slow (Abrol and Bhumbla, 1973). During leaching with water, the dissolution of calcite, gypsum and even silicate minerals (Rhoades et al., 1968) provide Ca source to replace Na. Hence this process depends on presence of Ca-bearing minerals in the soil.

Na removed from these columns was influenced by their initial Na concentration and SAR value. Analysis was performed after adjusting SAR covariate for Na leaching. The adjusted amount of Na leached are shown in Table 1.3. Analysis of covariance shows that none of the chemical treatments were effective in removing sodium from the Redfield column. These results are attributed to low Na concentration in these columns. In the White Lake columns, only two chemical treatments H_2SO_4 and $CaCl_2$ removed more sodium when compared to control (water) treatment. In this soil, gypsum did not accelerate Na loss. At Pierpont, all chemical treatments effectively removed more sodium from the soil. Others have reported mixed results (Sharma, 1971; Parther et al., 1978; Yahia et al., 1975). Differences in $CaSO_4$ and $CaCl_2$ as external Ca source to replace Na from the soil come from their difference in solubility. $CaCl_2$ being more soluble appeared to be more effective in Na removal than gypsum. The impact of H_2SO_4 on Na removal was attributed to it lowering the soil pH which solubilized $CaCO_3$. Others have reported that gypsum can be very effective. Sharma (1971) reported improved hydraulic conductivity and aggregate stability up to 30-cm depth by applying gypsum. Shanmuganathan and Oades (1983) reported that flocculating effect of gypsum is not only due to the replacement of Ca to Na but also due to the maintenance of electrolyte concentration in the soil system. Similar to our White Lake result, Parther et al. (1978) found more Na removed by H_2SO_4 treatment compared to gypsum treatment in calcareous sodic soil. Yahia et al. (1975) also showed more water penetration in columns treated with H_2SO_4 than gypsum.

Findings from this study suggest installing tile drainage will result in a decrease in soil EC, and that a portion of the cations leached from the soil will be Na. Decrease in soil EC however did not corresponded with the expectation of general rule of leaching hence further investigation is needed. Using chemical amendments along with leaching water enhanced the reclamation process. Sulfuric acid was a better chemical amendment at facilitating Na removal than $CaCl_2$ or gypsum.

Water permeability relationship with EC and SAR

Soil permeability is the ultimate test for sodic and saline-sodic soil management. Permeability on these soils is affected by salt (especially Na, Ca and Mg) concentration and composition. Several authors indicated Na to Ca ratio (Gardner et al., 1959; Quirk and Schofield, 1955; Shainberg and Caiserman, 1971; Pearson, 2009) is more important for water permeability. SAR is widely used index to characterize sodic soil and a soil with index value greater than 13 considered to be a sodic soil. Sodium can result in the swelling and dispersion of the clay platelets, which in turn reduces water permeability (McNeal et al., 1966). Other factors that can create unfavorable physical structure for permeability are soil texture, low organic matter, and high swelling-type clays (USSL, 1954).

For the columns collected at White Lake there was a good relationship between the soil initial SAR value and water permeability (mm/hr) (Fig. 1.2). The curve suggests that at a SAR value of 7 $mmol_c\ L^{-0.5}$ the permeability approached 1 mm hr^{-1}. Considering 1 mm hr^{-1} as a critical permeability (Sumner et al., 1998) this relationship suggests that the classification of sodic soils with SAR > 13 $mmol_c\ L^{-0.5}$ is not appropriate for NGP soils. Low SAR soil has shown a dispersive behavior in other studies too and hydraulic conductivity dropped to 1 mm hr^{-1} even at ESP value of 3-5 (McIntyre, 1979) in

Australian soil. That may be the reason why an ESP value 6 was used by Northcote and Skene (1972) to define sodic soils. Sumner et al (1998) explained two possible reason of these differences with USSL (1954) established ESP value 15 (or SAR 13 $mmol_c L^{-0.5}$), First, higher electrolyte concentration in water used to leach in California (3-14 $mmol_c L^{-0.5}$) compared to deionized water used in other studies, and second, lighter textured soil used in California compared to clay soil used in other studies.

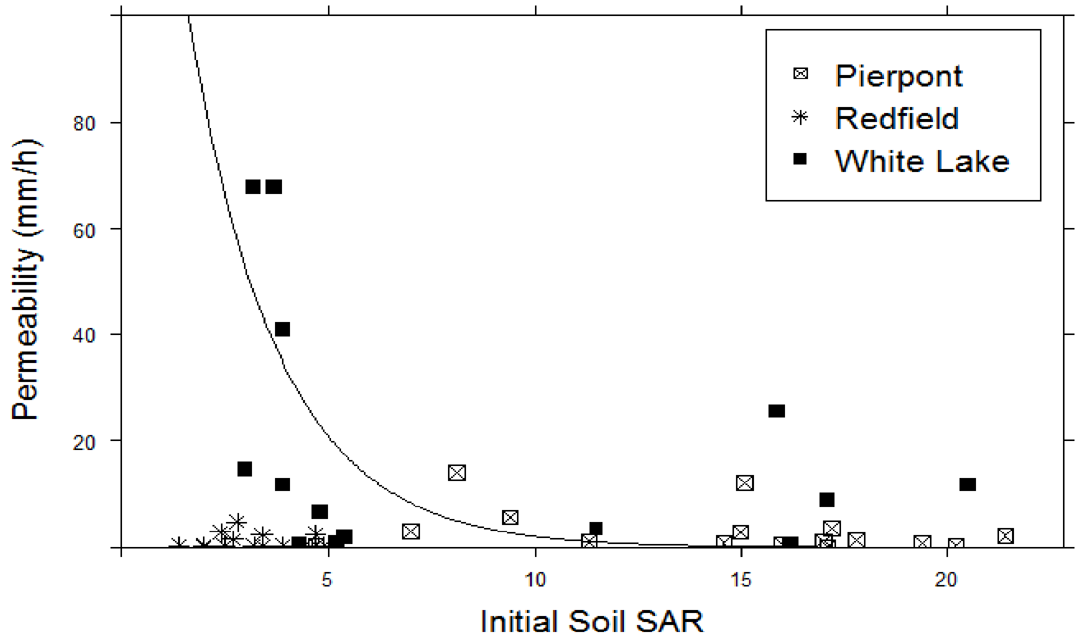

Figure 1.2 Permeability (mm/hr) as a function of initial soil SAR value

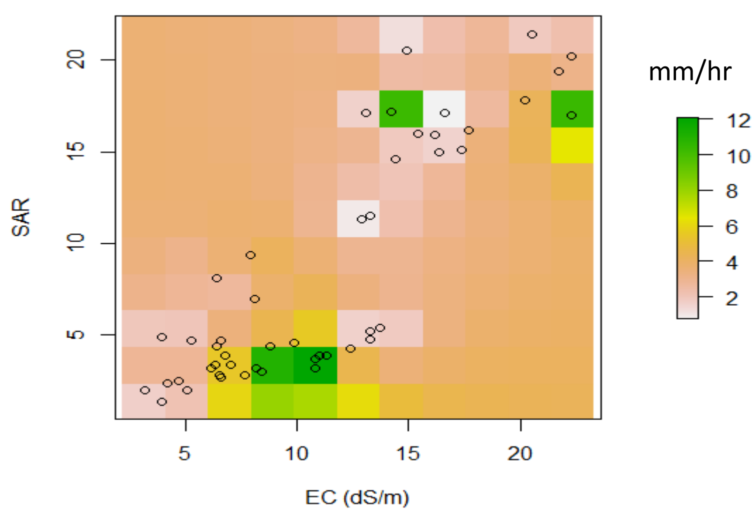

Figure 1.3 Water permeability (mm hr^{-1}) as affected by the soil column initial EC and SAR value.

Relationship between water permeability and SAR value differed for the three sites (Fig 1.2). These differences were attributed to differences in soil texture, organic matter, and the types of salts contained in the soil. Permeability as a function of both EC and SAR (Fig. 1.3) for all 3 sites combined did not show conclusive results. Several studies (USSL, 1954; Gardner et al., 1959) reported that ESP (or SAR) and EC interact on water permeability hence salinity classification adopted both EC and ESP in their definition. Shanmuganathan and Oades (1983) used ESP/EC ratio for their study and found dispersible clay content (%) increased linearly with increasing ESP/EC ratio in the soil. In our case, both permeability and EC value were divided by their respective SAR value. The relationship between these two parameters (Fig. 1.4) shows that permeability per unit of SAR increases with increasing EC to SAR ratio. Figure 1.4 further indicates that soil with EC to SAR ratio below 2 should be considered carefully for water permeability. Permeability itself is affected by several factors and if it is affected by SAR then the relation is a function of both EC to SAR ratio. Additionally this relationship is not a linear hence interpretation becomes difficult without additional analysis. Most of the soil with SAR values of 5 or greater showed relatively low EC to SAR ratio (Fig. 1.5A) in our study and these were the soils where water permeability management should be considered. Conversely, soil with less than 5 SAR value contained relatively higher EC to SAR ratio. Since this relationship came from 3 different locations with different soil types, this relation is explored more to make a general trend for the NGP soil.

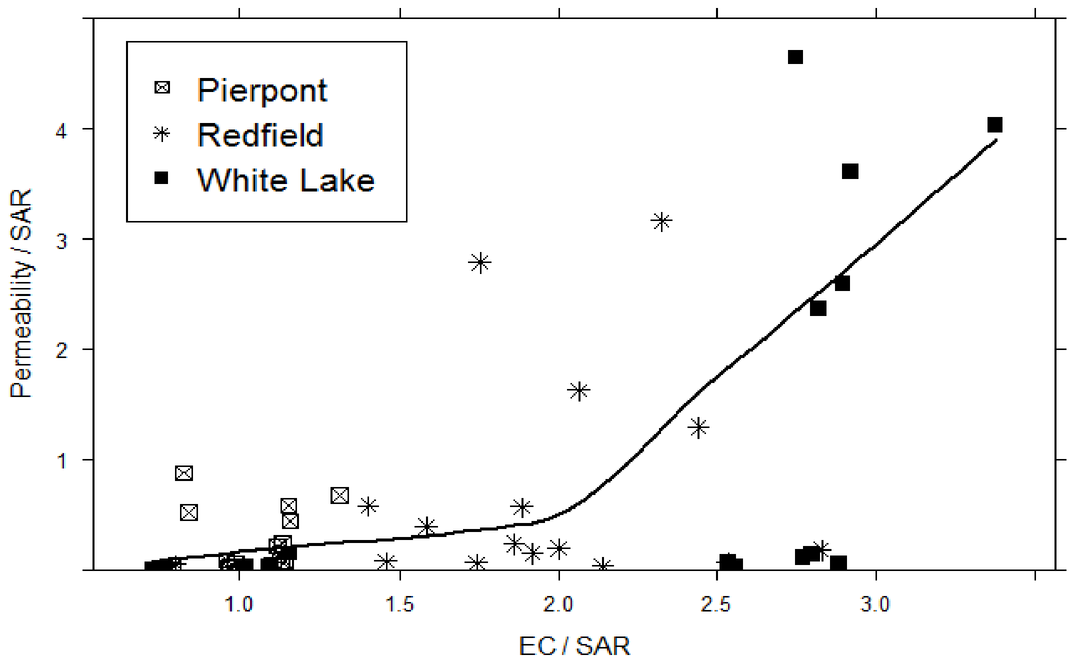

Figure 1.4 Water permeability per unit of SAR value as affected by the EC to SAR ratio.

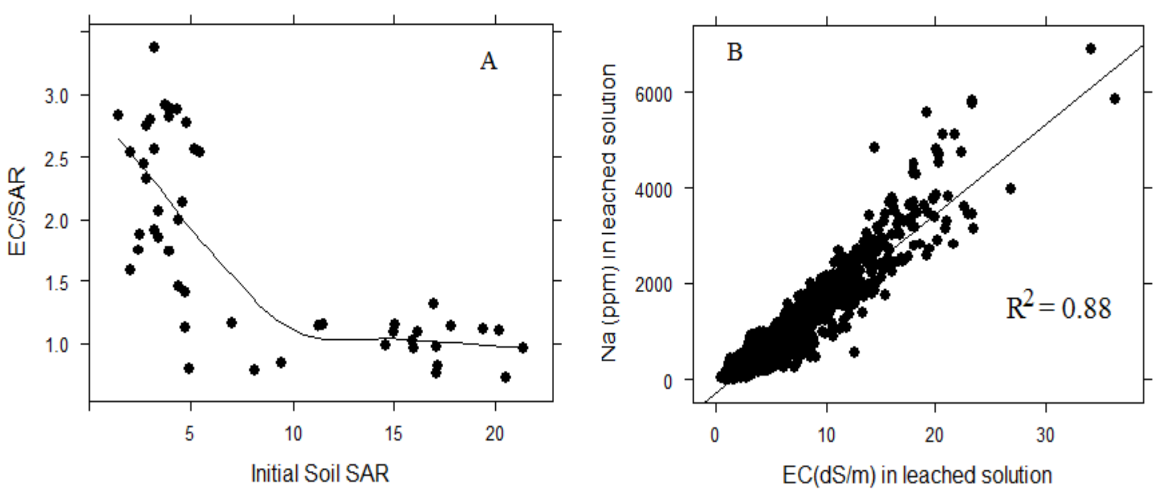

Figure 1.5 Relationship between A) soil EC to SAR ratio vs. soil SAR value, B) Na concentration (ppm) and EC (dS/m) of leaching solution. Data shown are for all 3 sites combined.

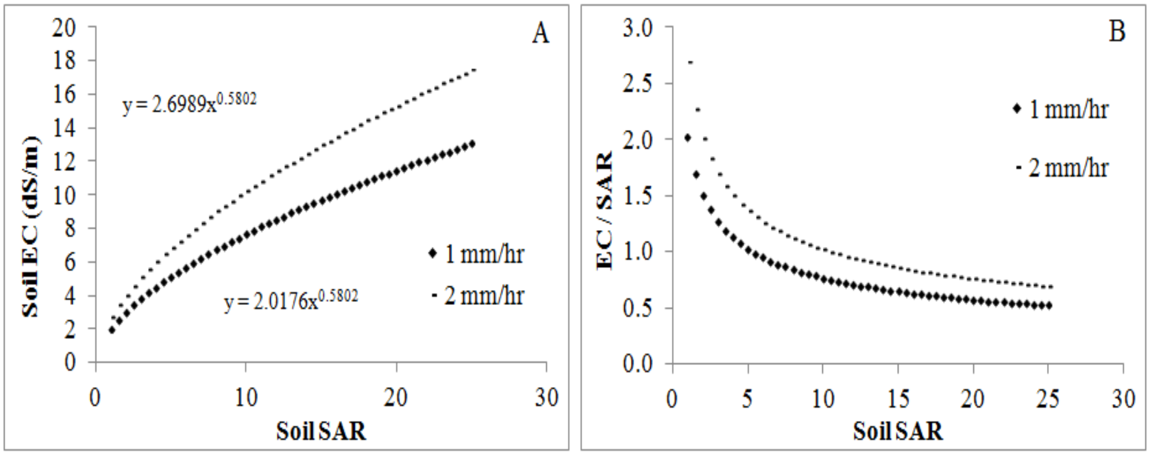

Figure 1.6 Required soil EC (A) and EC to SAR ratio (B) to maintain 1 and 2 mm/hr permeability at different soil SAR levels. Both EC and SAR were calculated as described in method section “Finding critical point of EC to SAR ratio”.

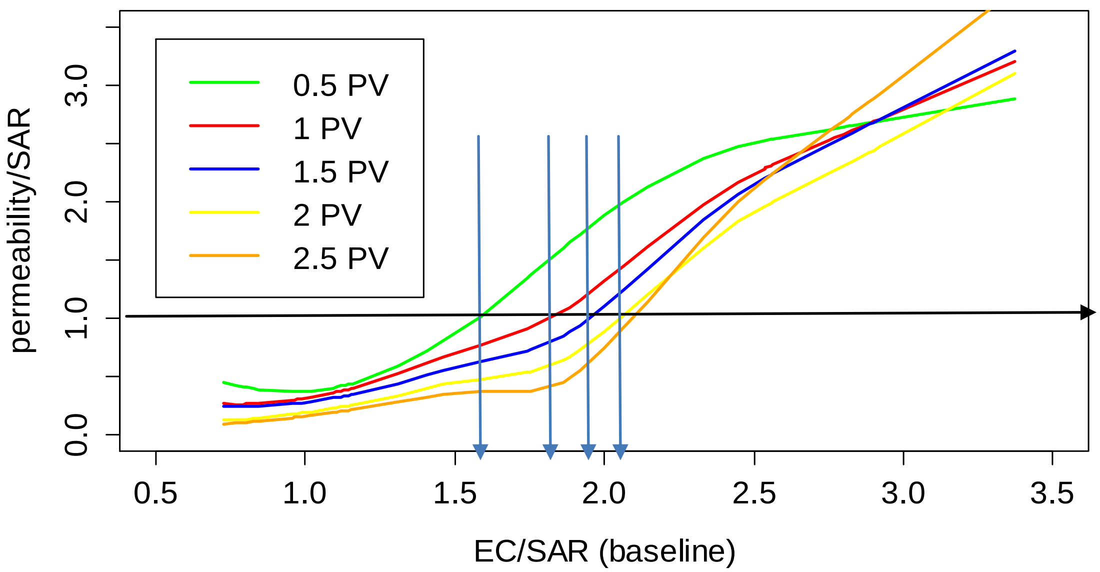

Figure 1.7 Water Permeability per unit of SAR as a response of soil EC/SAR ratio at different leaching period (1 PV = 11.3 cm water for Redfield and Pierpont site and 14.7 cm for White Lake Site)

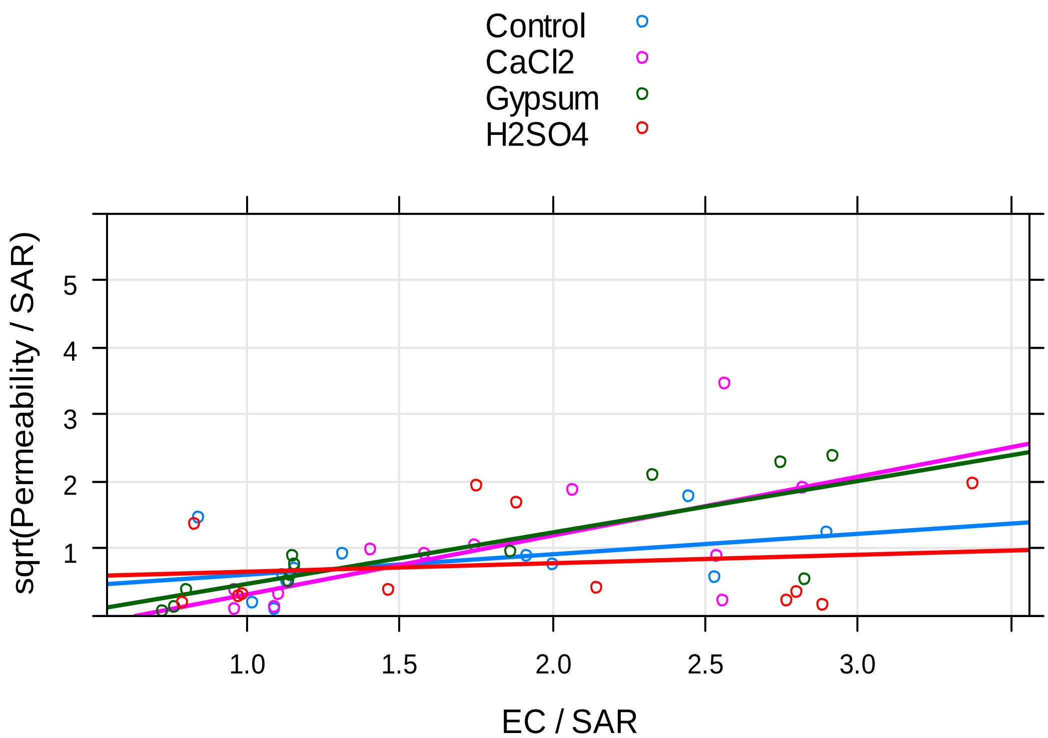

Figure 1.8. Salt treatment effect on water permeability at 2 pore volume of water leaching.

Critical EC to SAR ratio for water permeability

Soil EC required for each level of soil SAR to maintain critical water permeability were calculated. Resulting EC and SAR (Fig. 1.6 A and B) calculated for both 1 mm hr^{-1} and 2 mm hr^{-1} water permeability showed that EC to SAR ratio needed to maintain permeability were higher for soil with low SAR value and required EC to SAR ratio decreased with increasing SAR value. Additionally to maintain 2 mm hr^{-1} water permeability, EC to SAR ratio should be increased.

To maintain a water flow rate of 1 mm hr^{-1}EC to SAR ratio required was 2 for a soil with SAR value of 1 $mmol_c\ L^{-0.5}$. This ratio decreased to 1, 0.8 and 0.6 with SAR values of 5, 10 and 20 $mmol_c\ L^{-0.5}$, respectively (Fig 1.6B). Similarly, to maintain 2 mm hr^{-1} permeability, soil with 1 SAR required 2.7 times higher EC and it decreased to 1.4, 1.0 and 0.8 and with SAR value 5, 10 and 20, respectively. This decreasing trend of EC requirement with high sodium soil might be due to the solubility and availability of other salt species during sodium leaching process as shown in fig. 1.5B for EC and sodium content of leaching water.

These results show that soil permeability and soil EC to SAR ratio were related and to maintain permeability the ratio should be > 2. This can be achieved by adding Ca amendments if soil EC is lower than the required ratio. Additionally, our results showed that soil permeability decreased over time and that a higher EC/SAR ratio was needed to maintain permeability later in the leaching process (Fig. 1.7).

To assess how treatment affected water permeability behavior, data were again square root transformed to make relationship linear and graph was visually assessed.

Visually, two calcium source treatments (Gypsum and $CaCl_2$) were superior on maintaining water permeability compared to non Ca treatments (Fig. 1.8). These results are attributed to gypsum and calcium chloride providing a calcium source.

Conclusion

This study suggests that installing tile drainage will result in a decrease in soil EC, and that a portion of the cations leached from the soil will be Na. The relative loss of Na was dependent on soil structure. In soils with high amounts of Br remaining in the surface soil the EC/SAR ratio decreased. This decrease is attributed to an increase in the relative Na concentration, In soils with low amount of Br remaining in the surface soil, the EC/SAR ratio increased. This increase is attributed to an decrease in the relative Na concentration in the soil. Using chemical amendments along with leaching water enhanced the reclamation process as Na and other salts were removed. H_2SO_4 is the best amendment followed by $CaCl_2$ and gypsum to leach Na from the NGP region soil.

To maintain soil permeability, soil EC to SAR ratio should be considered. Most of the soil with low SAR (<5) in this region contained relatively higher EC to SAR ratio (>1.5) than the required ratio (>1) for effective water permeability. EC to SAR ratio of 1 was required to maintain electrolyte concentration by salt addition in soil with SAR value 5 and above. Ca source such as gypsum appears better to maintain required ratio.

References

Abrol, I. P., and D. R. Bhumbla. 1973. Leaching alone does not pay: apply gypsum in alkali soils. Indian Farm. 23:13-14.

Bresler, E., B.L. McNeal, and D.L. Carter. 1982. Saline and Sodic Soils, Principles-Dynamics-Modelling. Springer, Berlin Heidelberg New York.

Carlson, C.G., D.E. Clay, D. Malo, J. Chang, C. Reese, R. Owen, T. Kharel, and G. Birru. 2016. Saline (salts) and sodium problems and their management in dryland corn production. In: Clay, D.E., C.G. Carlson, S.A. Clay, and E. Byamukama (eds). iGROW Corn: Best Management Practices. South Dakota State University (under review).

Carlson, C.G., D.E. Clay, K. Reitsma, and R. Gelderman. 2013. Soybeans, salinity, and sodicity. Chapter 48. *In* Clay, D.E., C.G. Carlson, S.A. Clay, L. Wagner, D. Deneke, and C. Hay. (eds). iGrow Soybean: Best Management Practices. South Dakota State University

Carter, D.L., and C.D. Fanning. 1964. Combining surface mulches and periodic water applications for reclaiming saline soils. Soil Sci. Soc. Am. Proc. 28:564-567.

Carter, D.L., and C.W. Robbins. 1978. Salt outflow from new and old irrigated lands. Soil Sci. Soc. Am. J. 47:627-632.

Clay, D.E., Z. Zheng, Z. Liu, S.A. Clay, and T. P. Trooien. 2004. Bromide and nitrate movement through undisturbed soil columns. J. Environ. Qual. 33:338-342.

Custer, S. 1976. The nitrate problem in areas of saline-seep-A case study. Regional Saline Seep Control Symposium Proceedings, Montana State Univ., Cooperative Extension Service Bul. 1132:63-85.

Flury, M.,. H. Fluhjler, AW.A. Juay, and J. Leuenberger. 1994. Susceptibility of soil to preferential flow of water: A field study. Water Resource Res. 30:1945-1954.

Franzen, D.W., and J.L. Richardson. 2000. Soil factors affecting iron chlorosis of soybean in the Red River Valley of North Dakota and Minnesota. J. Plant Nutr. 23: 67-78

Gardner, W.R., M.S Mayhug, J. O. Goertzen, and C.A. Bower. 1959. Effect of electrolyte concentration and exchangeable sodium percentage on diffusivity of water in soils. Soil Sci. 88:270-274.

Hadrich, J. 2012. Managing the economics of soil salinity in the Red River Valley of North Dakota. J. American Society of Farm Managers and Rural Appraisers. p. 80-88. http://purl.umn.edu/190726

Hatfield, J.L., K.J. Boote, B.A. Kimball, L.H. Ziska, B.C. Izauralde, D. Ort, A.M. Thomson, and D. Wolfe. 2011. Climate impacts on agriculture implications of crop production Agron. J. 103:351-370.

Hopkins, D., K. Chambers, A. Fraase, Y. He, K. Larson, L. Malum, L. Sande, J. Schulte, E. Sebesta, D. Strong, E. Viall, and R. Utter. 2012. Evaluating salinity and sodium levels on soils prior to drain tile installation: a case study. Soil Horizons 53:24-29.

Jury, W.A., W.M. Jarrell, and D. Devitt. 1979. Reclamation of saline-sodic soils by leaching. Soil Sci. Soc. Am. J. 43:1100-1106.

Kunkel, K. E., L. E. Stevens, S. E. Stevens, L. Sun, E. Janssen, D. Wuebbles, M. C. Kruk, D. P. Thomas, M. D. Shulski, N. Umphlett, K. G. Hubbard, K. Robbins, L. Romolo, A. Akyuz, T. Pathak, T. R. Bergantino, and J. G. Dobson, 2013: Regional Climate Trends and Scenarios for the U.S. National Climate Assessment: Part 4. Climate of the U.S. Great Plains. NOAA Technical Report NESDIS 142-4. 91 pp., National Oceanic and Atmospheric Administration, National Environmental Satellite, Data, and Information Service, Washington, D.C. (http://www.nesdis.noaa.gov/technical_reports/NOAA_NESDIS_Tech_Report_142-4-limate_of_the_U.S.%20Great_Plains.pdf)

McCombie, B. 2009. 911 for CRP: what will be the fate of America's most successful wildlife habitat program? Outdoor Life (May):27-28

McIntyre, D. S. 1979. Exchangeable sodium , subplasticity and hydraulic conductivity of some Australian soils. Aust. J. Soil Res. 17:115-120.

McNeal, B.L., W.A. Norvell, and N.T. Coleman. 1966. Effect of solution composition on soil hydraulic conductivity and on the swelling of extracted soil clays. Soil Sci. Soc. Am. Proc. 30: 308-317.

Millar, J.2003.Managing Salt affected soil. SD No-till Newsletter.Available: http://www.sdnotill.com/Newsletters/2003_Salt_Soils.pdf

Northcote, K.H., and J. K. M. Skene. 1972. Australian soils with saline and sodic properties. Soil Publ. 27. CSIRO Publ. Melbourne, Australia

NRCS. 2012. Economic impact of saline soils in Upper James River. SD-FS-81.available at http://www.nrcs.usda.gov/Internet/FSE_DOCUMENTS/nrcs141p2_035584.pdf

Oster, J.D., and G. Sposito.1980. The gapon coefficient and the exchangeable sodium percentage-sodium adsorption ratio relation. Soil Sci. Soc. Am. J. 44: 258–260

Overstreet, R., J.C. Martin, and H.M. King. 1951. Gypsum, sulfur and sulfuric acid for reclaiming an alkali soil of the Fresno series. Hilgardia. 21:113-127

Parther, R. J., J.O. Goertzen, J.D. Rhoades, and H. Frenkel. 1978. Efficient amendment use in sodic soil reclamation. Soil Sci. Soc. Am. J. 42:782-786.

Pearson, K.E., 2009. The basics of salinity and sodicity effects on soil physical properties. Montana State University. Available at http://waterquality.montana.edu/docs/methane/basics_highlight.shtml

Quirk, J. P., and R. K. Schofield. 1955. The effect of electrolyte concentration on soil permeability. J.Soil Sci. 6:163-178.

R Core Team. 2015. R: A language and environment for statistical computing. R Foundation for Statistical Computing, Vienna, Austria. (https://www.R-project.org)

Reistma, K.D., B.H. Dunn, U. Mishra, S. A. Clay, T. DeSutter, and D. E. Clay. 2015. Land-use change impact on soil sustainability in a climate and vegetation transition zone. Agron. J. 107: 2363-2372.

Rhoades, J. D, D.B. Krueger, and M.J. Reed. 1968. The effect of soil-mineral weathering on the sodium hazard of irrigation waters. Soil Sci. Soc. Am. J. 32:643-647.

Rhoades, J. D., and A. D. Halverson. 1976. Detecting and delineating saline seeps with soil resistance measurements. Regional Saline Seep Control Symposium Proceedings, Montana State University, Cooperative Extension Service Bul. 1132, 19-34.

Schrag, A.M. 2011. Addendum: climate change impacts and adaptation strategies. *In* Forrest, S.C., H. Stand, W.H. Haskins, C. Freese, J. Proctor, and E. Dinerstein (eds.). Ocean of grass: A Conservation Assessment for the Northern Plains Conservation Network and Northern Great Plains Ecoregion. World Wildlife Fund-US, Bozeman MT, Available athttp://kresge.org/sites/default/files/Uploaded%20Docs/WWF%20-%20Ocean_Grass.p

Seelig, B,D., 2000. Salinity and sodicity in North Dakota soils. NDSU Extension. http://www.ndsu.edu/soilhealth/wp-content/uploads/2013/03/ND-saline-sodic-soils_2000.pdf.

Shafer, M., D. Ojima, J. M. Antle, D. Kluck, R. A. McPherson, S. Petersen, B. Scanlon, and K. Sherman, 2014: Ch. 19: Great Plains. In: Climate Change Impacts in the United States: The Third National Climate Assessment. J. M. Melillo, Terese (T.C.) Richmond, and G. W. Yohe, Eds., U.S. Global Change Research Program, 441-461. doi:10.7930/J0D798BC (http://nca2014.globalchange.gov/report/regions/great-plains)

Shainberg, I., and A. Caiserman. 1971. Studies on Na/Ca montmorillonite systems: II. The hydraulic conductivity. Soil Sci. 111:276-281.

Shanmuganathan, R. T., and J. M. Oades. 1983. Modification of soil physical properties by addition of calcium compounds. Aust. J. Soil. Res. 21: 285-300.

Sharma, M. L. 1971. Physical and physico-chemical changes in the profile of a sodic soil treated with gypsum. Aust. J. Soil Res.9:73-82

Soil Survey Staff, Natural Resources Conservation Service, United States Department of Agriculture. Web Soil Survey. Available online at http://websoilsurvey.nrcs.usda.gov/. Accessed [5/30/2015].

Sumner, M. E., P. Rengasamy, and R. Naidu. 1998. Sodic Soils: A Reappraisal. In: Sodic Soils: Distribution, Properties, Management and Environmental Consequences. Eds. M. E. Sumner, R. Naidu. Oxford University Press. Oxford, New York.

U.S. Salinity Laboratory Staff. 1954. L.A. Richards (ed.) Diagnosis and Improvement of Saline and Alkali Soils. USDA Agric. Handb. 60. U.S. Govt. Print. Office, Washington, DC.

Warncke, D. and J.R. Brown. 2015. Potassium and other basic cations. In: Recommended Chemical Soil Test Procedures for the North Central Region. NCR Publication No. 221(Revised). Missouri Agricultural Experiment Station, Columbia, MO, USA.

Whitney, DA. 2015. Soil Salinity. In: Recommended Chemical Soil Test Procedures for the North Central Region. NCR Publication No. 221 (Revised). Missouri Agricultural Experiment Station, Columbia, MO, USA.

Yahia, T. A., S. Miyamoto, and J.L. Stroehlein. 1975. Effect of surface applied sulfuric acid on water penetration into dry calcareous and sodic soils. Soil Sci. Soc. Am. Proc. 39:1201-1204.

Chapter 2

The development and use of a remote sensing soil salinity model for assessing salinity changes in South Dakota

Summary

Increasing temperature and precipitation are the major factors contributing to the expansion of the Northern Great Plains saline and sodic soils. The objective of this study was to develop a remote-sensing model that can be used to identify the extent of this growing problem. Soil samples from 0- to15- cm depth in 62 x 62 m grid spacing were taken from Pierpont (65 ha) and Redfield (17 ha) sites in South Dakota. The saturated paste EC vales were measured on these soil samples. At each sampling points reflectance and derived indices (Landsat 5, 7, 8 images), elevation, slope and aspect (LiDAR) were extracted. Multiple linear regression, classification and regression tree, cubist, and random forest method were compared for soil EC prediction. Random forest method was found to be the most effective method because of its ability to capture spatially correlated variation. Results show that short wave infrared, SWIR (1.5 -2.29 µm) bands (B5 and B7 in Landsat 7 and Landsat 5, and B6 and B7 in Landsat 8) and near infrared, NIR band (B4 in Landsat 5) were sensitive with soil salinity. Soil EC were predicted using spring, summer, fall or a combination of the three season imagery showed that predicted EC was influenced by sampling date and crop type. Soil EC predicted using multi-year spring images showed higher R^2 (0.56) value with specific field validation data set (Redfield), whereas EC predicted using all 3 season images showed better R^2 (0.26) with the state wide validation data set. In South Dakota, the model predicted that from 2008 to 2012,

the soil EC values increased in 569,200 ha or 13.4% of the land seeded to corn or soybeans.

Introduction

Worldwide, balancing food and energy production is a complex problem because, depending on the region, climate oscillations may positively or negatively impact climatic risks. The problem is confounded by a shrinking land base for producing food. For example, according to the USDA NASS, 30 million ha of US farmland were taken out of production between 1990 and 2012. Reduction in farmland acres intensifies the demands on all current farmland, just to replace products from those areas, let alone boost outputs to nourish an increasing global population. In the NGP, climate change has increased spring rainfall and temperatures, making the growing of annual crops less risky (Schrag, 2011; Clay et al., 2014; Cook et al., 2015; Reitsma et al., 2015). However, associated with the reduced risk of drought is an increased erosion risk. In NGP landscapes, greater rainfall causes water tables to rise, which enables sodium (Na^+) and other salts contained in subsoil marine sediments, to be transported with capillary water to the soil surface. Over time, small problem areas can become large expanses.

In the NGP, it is estimated that 10.6 million hectares of Minnesota (20,100 ha), Montana (4,380,000 ha), Nebraska (56,800 ha), North Dakota (2,350,000 ha), South Dakota (3,442,000 ha) and Wyoming (445,344 ha) land are impacted by saline conditions (Schrag, 2011; Cook et al., 2015; Seelig, 2000; Millar, 2003; Hopkins et al., 2012; Carlson et al., 2013), and over 2 million hectares of land are impacted by high Na concentrations in South Dakota (1,200,000 ha) and North Dakota (800,000ha) (Millar, 2003; Seelig, 2000). Worldwide, salinization and sodification are often linked to irrigation, whereas in South Dakota and North Dakota the expanding problem is associated with increasing spring precipitation, higher temperatures and capillary rise of salts to the rooting zone.

Globally, saline and Na^+ effected soils are separated into at least three groups: saline (high total salts), saline/sodic (high total salts and Na^+), and sodic (high Na^+) (Rhoades and Halverson, 1976). The classification of a salt-affected soil into one of these groups is based on the soil electrical conductivity (EC) and the amount of Na^+ on the cation exchange sites. Sodic soils are characterized as having a Na^+ adsorption ratio (SAR) > 13 $mmol_c\ L^{-0.5}$, whereas in the NGP, soils are at risk when the SAR increases above 5 $mmol_c\ L^{-0.5}$ (He et al., 2015a, 2015b). Suarez et al. (2008) had similar results for irrigated systems in California and reported that infiltration decreased as SAR increased from 2 to 4 $mmol_c\ L^{-0.5}$.

The traditional approach to remediate a saline/sodic soil in the arid, irrigated regions of the Southwestern United States is to: 1) apply water with a low electrical conductivity (EC), 2) add a source of calcium (gypsum, lime), and 3) allow for adequate drainage, which is most commonly done by installing tile drainage (Seelig, 2000, Carlson et al., 2013; Hopkins et al., 2012; He et al., 2014). However, in semi-arid non-irrigated systems, such as those observed in the NGP and Australia, these remediation steps may actually worsen the problem (Northcote and Skene, 1972; McIntyre, 1979). The failure of traditional salt-affected soil best management practices (BMP) in dryland systems are attributed to the failure to account for differences in the EC values of water leaching through the soil, differences in soil texture, and the failure to consider the water cycling across the topographic relief (Sumner et al., 1998; Suarez et al., 2008).

Figure 2.1 The effects of 'traditional' remediation of salt-affected soils in the NGP. After drainage was implemented, gully formation can be observed after 2.5 cm of rainfall (right) and the topsoil became dispersed (left). Sediment and excess agrochemicals are transported to stream, rivers, and the atmosphere. Farmers consider this problem as an economic loss, while environmentalists would assess such events as preventable tragedies.

These fragile salt-affected soils often found in riparian zone near streams and river. Within agricultural field, the lower lying landscape positions are developing to the saline/sodic soil. Sparse plant growth on these saline/sodic soils, when combined with high water flow with destabilized soil aggregates, results in silt-laden runoff (Fig 2.1). Sediments (sand, silt and clays) may settle in region's hydroelectric power reservoirs and affect local infrastructure. Salts are transported much further and may impact water quality used for several purposes such as drinking, irrigation, recreation and aquatic habitat along the lengths of the Missouri and Mississippi river systems, and into the Gulf of Mexico. Locally, the economic consequences of saline soils are staggering. Due to high salt concentrations [EC≥ 4 dS/m], the economic loss on 113,000 ha in SD Beadle, Brown, and Spink counties has been estimated at $26.2 million per year (NRCS, 2012), and in North Dakota's Red River Valley, the loss is estimated at $150 million per year (Hadrich, 2012).

One of the consequences of saline and sodic soil development is the creation of soil profiles which change soils reflectance characteristics (Schmid et al., 2009; Rao et al., 1995; Joshi et al., 2002). However, depending on the magnitude and cause of the problem, different reflectance characteristics are possible. In an extreme condition, salt accumulations can result in a white crust on the soil surface. Under these conditions soils with a mineral crust have 70 to 90% reflectance in the 500- to 1,000- nm wavebands (Howari et al., 2002). However, the degree of reflectance is influenced by the mineral composition. For example, gypsum had a lower reflectance than calcite in the 1,500-, to 2500- nm wave bands. Other studies (Nawar et al., 2014; Metternicht and Zinck, 2003;

Schmidt et al., 2009; and Sidike et al., 2014) showed that reflectance decreased with salinity and sodicity.

Soil EC prediction using Landsat images is the continuation of the classical model of soil (Jenny, 1941) modified to accommodate new information and tools available today (McBratney et al., 2003; Lobell et al., 2015). Different layers of indirect soil information are used to predict particular soil property such as soil EC. Since spatial resolution of model inputs are very detailed compared to classical soil map developed for each mapunit, output will be a valuable information for land managers.

In summary, researchers have used variety of remote sensing data and techniques to assess and map soil salinity. Recent work in Red River valley, North Dakota indicates that long term vegetation index (EVI and NDVI) can be used to assess soil salinity (Lobell et al., 2010). Their work involved for regional scale soil salinity assessment using moderate resolution imaging spectroradiometer (MODIS) imagery. For the field scale I hypothesize that using long term spring season Landsat imagery when soil is covered minimally with the vegetation will be a more direct method to assess soil salinity. I tested this hypothesis using variety of machine learning techniques. Overall objective of this study is to develop a remote sensing model that can be used to identify the extent of this growing saline problem in the Northern Great Plains.

Materials and Methods

Sample collection and processing

Two sites, Pierpont (45.4751° N, 97.8359° W, 65 ha) and Redfield (44.9250° N, 97.4760° W, 17 ha) were selected for this study. The soils at both sites were formed on glacially deposited parent materials that overlaid marine sediments. The soil textures at the sites ranged from silt loams to silty clays, and the slope ranged from 0- to 9-% at Pierpont and from 0- to 6- % at Redfield.

Soil samples (0-to 7.5- and 7.5- to 15- cm) were collected from a 62 by 62 m grid in November and July 2013 from Pierpont and Redfield sites, respectively. Each sample consisted of composite of 15 cores that were randomly collected from a 1 m^2 sampling area. At Pierpont, 204 samples were collected, whereas at Redfield, 41 samples were collected. Coordinates of all sampling points were located with a differentially corrected global positioning system (DGPS).

Soil samples were air dried (40° C), ground, and sieved through 2 mm screen. Approximately 150 cm^3 of Type I (high purity deionized nanopure) water was added to 250 g of ground soil to make saturated paste. The saturated pastes were equilibrated for > 8 hours before soil solution extraction. The soil EC (dS/m) of the solution extract was measured with a conductivity probe (PC 2700, Oakton Instruments, Vernon Hills, IL), and the concentration of Na^+, Ca^{2+}, and Mg^{2+} were measured using flame atomic adsorption spectrophotometry (200 A, Buck Scientific, Norwalk, CT). For Na^+ and Mg^{2+} analyses the samples were diluted using a calcium suppressant solution ($La_2O_3 \cdot HCl$

solution) (National Soil Survey Center, 1996). Sodium adsorption ratios (SAR) were calculated using Equation 1.

$$SAR = \frac{[Na^{+}]}{\left(\frac{[Ca^{2+}] + [\mathrm{Mg}^{2+}]}{2}\right)^{1/2}} \qquad [1]$$

Based on the soil EC, the soil samples were separated into 5 categories (<2, 2-4, 4-10, 10-20 and >20 dS/m), and based on the SAR values, the samples were separated into 4 categories (<4, 4-6, 6-13 and >13 $\mathrm{mmol_c\ L^{-0.5}}$). Summary statistics of these data are provided in Table 2.1.

For model validation, a set of 65 soil samples from the 0- to 15- cm were randomly collected from 8 different sites of eastern South Dakota (Fig. 2.2). Processing and analysis followed the procedures described above.

As a secondary validation, gridded soil survey geographic (gSSURGO) data from natural resource conservation service (NRCS), US Department of Agriculture was used. Saturated paste soil EC from SSURGO data were first aggregated for each map unit and then extracted for 3730 data points across eastern South Dakota.

Table 2.1 Summary statistics of soil grouping for EC and SAR from Pierpont, SD.

Salinity	# sample	Mean	CI(95%)*	Elevation	Slope	Moisture
EC	N	EC(dS/m)	EC(dS/m)	m	%	%
EC0-2	81	0.82	0.10	420. 0	1.30	28.4
EC2-4	48	3.00	0.15	417.7	1.58	30.2
EC4-10	32	5.64	0.51	416.6	1.37	31.2
EC10-20	12	13.16	1.70	416.1	1.70	27.8
EC20-42	31	28.62	1.71	415.5	2.35	35.0
SAR		SAR	SAR			
SAR0-4	142	1.42	0.17	418.9	1.41	25.4
SAR4-6	18	4.84	0.31	416.1	1.78	27.2
SAR6-13	34	8.72	0.66	416.1	1.91	29.4
SAR13-43	10	22.30	6.80	416.0	2.18	34.9

*CI= Confidence Interval at 95%

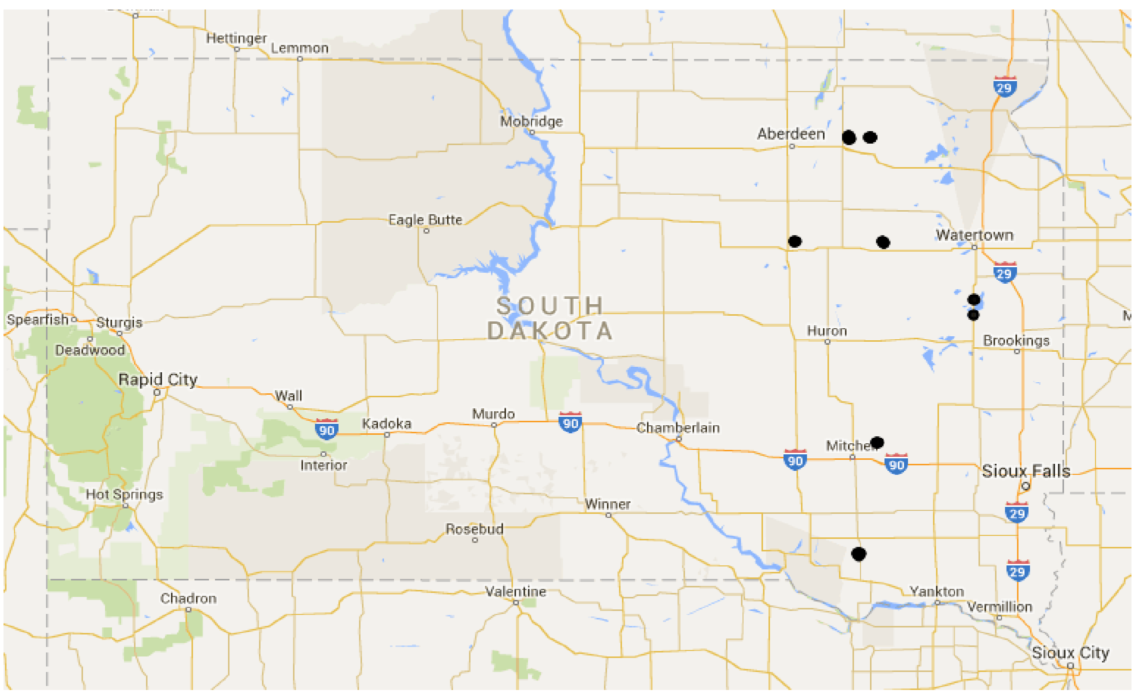

Figure 2.2 Sixty five validation samples collected from 8 eastern sites of South Dakota. At each site, samples were collected to represent gradient of soil salinity along the landscape.

Ground based reflectance and moisture sensing

At Pierpont, the surface soil (0-6 cm) moisture at each sampling point was measured on 17 May 2014 using a handheld soil moisture meter ML3 ThetaProbe (TH2O Theta soil moisture meter, Dynamax, Houston, TX). This instrument measured volumetric soil moisture content using dielectric constant of mineral soil. Simultaneous to the soil moisture measurements, surface soil reflectance was measured using a multispectral radiometer (MSR16R Crop Scan unit, Crop Scan Inc., Rochester, MN). The Crop Scan simultaneously measured reflected and incoming energy in 450- to 1750- nm range. Reflectance was measured between 1100 and 1400 hours (Chang et al., 2004). At each sampling points, 3 readings were collected and averaged.

Model building process using Landsat 8 and DEM image

Landsat 8 operational land imager/thermal infrared sensors (OLI/TIRS) images (2013 and 2014) with <30% cloud cover were obtained for Pierpont and Redfield site. Digital reflectance values for the thermal infrared (TIRS) band 10 (10.60 – 11.19 µm) and band 11 (11.50 -12.51 µm) were converted to top of atmosphere (TOA) radiance using "rLandsat8" package in R. The reflectance and radiance values, from each of the soil sampling points, were combined with elevation, slope and aspect information derived from a light detection and ranging (LiDAR) digital elevation model. Sampling points were randomly split into 134 points for model development and 70 points for model validation. Multiple linear regression, classification and regression tree, cubist and random forest methods were used for model development and comparisons.

Classification and Regression Tree (CART), introduced by Breiman et al. (1984) is a statistical data mining technology. It divides data based on binary recursive partitioning method and is not affected by non-linearity in data structure. Breiman et al. (1984), and Steinberg and Colla (1995) provide the details of these methods. Cubist and Random forest methods are extension of the regression and classification method. Random Forest is specifically suitable for small number of observations with large number of variables (small n large p), high order interaction and correlated variables. Several authors used these method to estimate crop yield and soil properties (Pachepsky et al., 2001; Shatar and McBratney, 1999; Howari, 2003; Masoud and Koike, 2006)

After developing these machine learning algorithms for soil EC, models were compared using coefficients of determination (R^2), mean square error (MSE) and semivariance of the model residuals. The R^2 and MSE values are a measures on the strength of the relationship between the measured and predicted values. Semivariance of model residual provides an assessment of the models ability to remove spatial correlation. Unlike random variables, regionalized variable such as soil electrical conductivity exhibit spatial continuity (Webster and Oliver, 2001) and this can be assessed by semivariogram. Semivariogram is a plot of the semivariance of a property (regionalized variable) over a set of distances called lag. Semivariance measures dissimilarity of a property over a range of distance. In our case soil EC was spatially correlated up to 200 m.

Time series of Landsat 7 and Landsat 5 images

Time series image of Landsat 7 and Landsat 5 were used for two separate assessment purpose. First, images from 1999 to 2015 were used to identify best responsive bands to soil EC. For this purpose, soil data were grouped low to high EC into

5 categories (<2, 2-4, 4-10, 10-20 and >20 dS/m) and time series of reflectance on those sampling points were analyzed. For the older images, they were calibrated using Chander et al. (2009) and for the newer images they were calibrated using coefficients provided with image metadata (Google Earth Engine Team, 2015). Time series data were statistically analyzed for monotonic trend using Mann-Kendall test. This test is non-parametric and does not require residuals to be normally distributed. This test assesses if a variable is monotonically going upward or downward over the time period even though the trend may or may not be linear.

Second, Landsat 5, 7 and 8 TOA images from 2005 to 2013 were used to track changes in soil EC over time. Less than 30% cloud covered images for three time periods (April-May as a spring image, June-August as a summer image, and September-October as a fall image) were used for this purpose. These three time periods represent three growth periods (growth initiation, vegetative growth and reproductive/maturity stages). For each growth period, 3-year median values of reflectance and vegetation indices (Table 2.2) image were created. For example, spring median image for 2008 were created from the all cloud free images available during spring season from 2007 to 2009. Soil EC was predicted using 3 year median images with the random forest model. A planetary scale mapping platform Google Earth Engine API was used at this stage. Predicted EC and change was assessed using the eastern South Dakota landuse change data set (Reistma et al., 2015). A total of 3,733 data points corresponding to cropland both in 2006 and 2012 were used for this purpose. For each point, growing season (April 1 - September 30) total precipitation (mm), maximum and minimum temperature (ºK) and soil properties were extracted. Gridded surface meteorological data (GridMet) from

University of Idaho was used for precipitation and temperature extraction while gridded soil survey geographic (gSSURGO) database from NRCS was used for soil properties. Finally, all the points were grouped based on land capability class (LCC) for summary statistics.

Table 2.2 Reflectance indices used for soil salinity prediction

Indices used for this study
Normalized difference moisture index, NDMI = (SWIR - NIR)/(SWIR+NIR)
Normalized difference vegetation index, NDVI = (NIR-R)/(NIR+R)
Normalized difference water index, NDWI = (NIR-Green)/ (NIR + Green)
Mid Infrared Burn Index, MIRBI= (10*B7) - (9.8* B6) + 2.00
Salinity Index (Landsat8), SI = $\sqrt{B2 * B4}$
Normalized difference Salinity Index, NDSI = (B4 - B5)/ (B4 + B5)
Brightness Index, BI = $\sqrt{B4^2 + B5^2}$
Soil Adjusted Vegetation Index, SAVI = 1.5[(NIR - RED) / (NIR + RED + 0.5)]

Results and Discussions

Reflectance characteristics over EC and SAR range

Surface reflectance decreased with increasing salinity (Fig. 2.3A). This is in contrast to other studies that reported the contrary (Schmid et al., 2008; Rao et al., 1995, Joshi et al., 2002). In the NGP, several factors may be responsible for the differences. First, soils with high salinity are often found in footslope areas where the soil moisture content may be very high. Since water absorbs more and reflects less light compared to bare soil, we can expect lower reflectance in lower part of the landscape (footslope and toeslope). To verify if the difference in reflectance was attributed to differential soil moisture, the soil moisture content of the different EC classes were compared. This analysis suggests that on May 17, the moisture content of soils with EC < 20 dS/m were similar (Fig. 2.4, Table 2.1). Soils with EC>20 dS/m had higher soil moisture contents and were generally located in footslope areas (Table 2.1). In all of the soils, white salts were generally not present on the soil surface.

Landsat-8 reflectance values were lower than MSR-Crop Scan reflectance value (Fig. 2.3A and B). This could have due to differences in sensors (Nawar et al., 2014) and atmospheric distortion as Landsat 8 image used were top of atmosphere reflectance or it could be due to other factors since these two readings were taken a month apart. Both Landsat-8 and MSR-Crop scan data indicate that reflectance decreased with increasing salinity. Nawar et al (2014) showed similar trend in field soil reflectance using portable spectroradiometer (FieldSpec-FR, ASD) and Landsat-7 ETM+ over EC range 3.8 to 58.6 dS/m. Similar results are shown by Metternicht and Zinck (2003), Schmid et al. (2009), and Sidike et al. (2014).

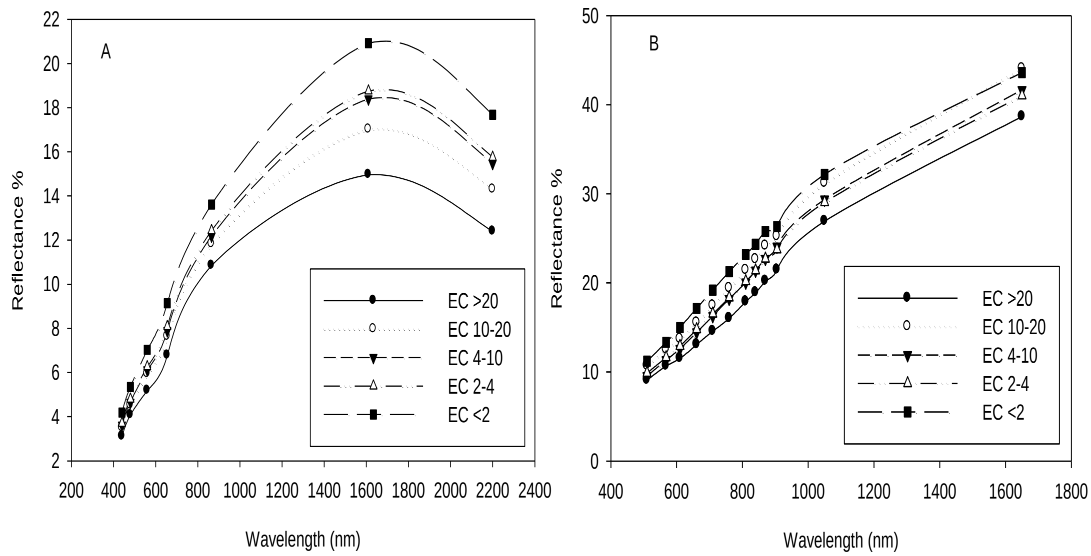

Figure 2.3 Surface reflectance, A) April 17, 2014 Landsat 8, and B) May 17, 2014, MSR-CropScan as affected by soil electrical conductivity (EC) levels at Pierpont site.

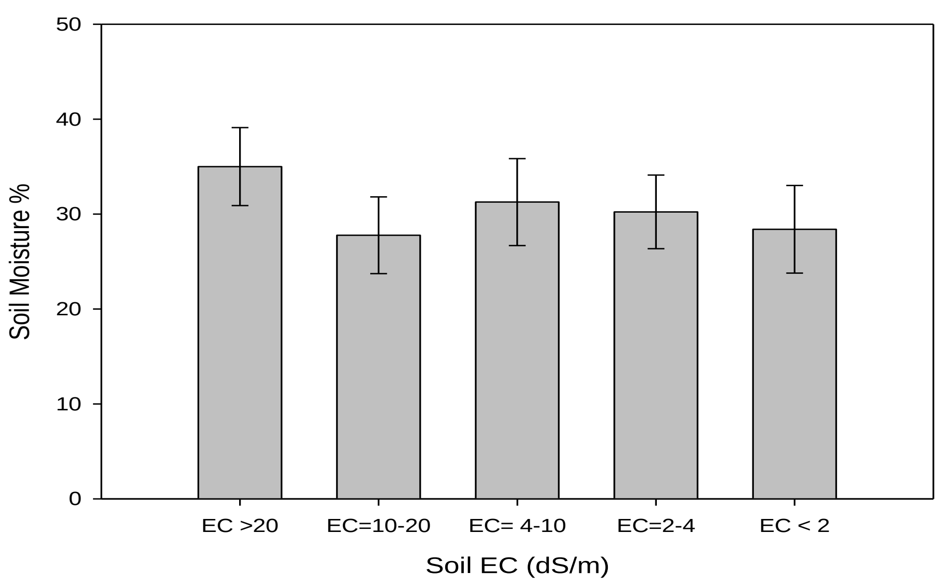

Figure 2.4 Volumetric soil moisture content (6 cm depth) recorded on May 17, 2014 at Pierpont site shows slightly higher moisture content at grid points with EC>20, but there was no difference in moisture content in other grid points.

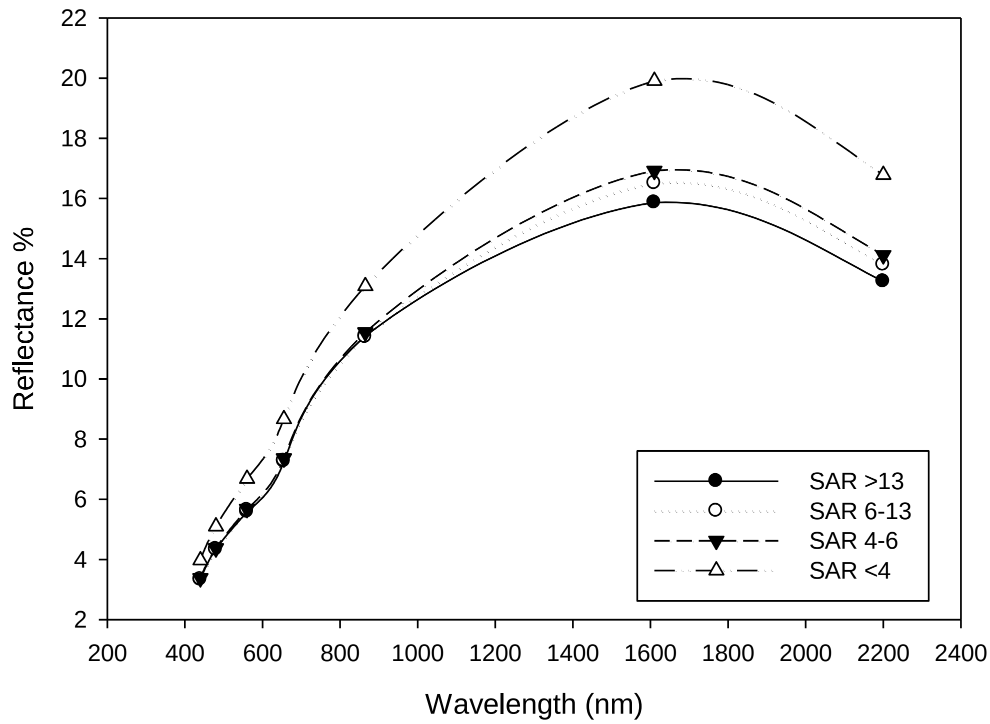

Figure 2.5 Surface reflectance (April 17, 2014 Landsat-8) as affected by Sodium Absorption Ratio (SAR) levels at Pierpont site.

Reflectance was higher when soil SAR was low (Fig. 2.5). These results indicate that reflectance of soil with a SAR value <4 $mmol_c\ L^{-0.5}$ is very different than soil with a SAR > 4 $mmol_c\ L^{-0.5}$. Reflectance decreased 11- to 16-% from soil with SAR < 4 $mmol_c\ L^{-0.5}$ to soils with SAR values between 4- to 6- $mmol_c\ L^{-0.5}$. Reflectance decreased further with higher SAR soil value but this decrease was subtle, ranging only 0.31 -2.2 % across the bands.

Correlation analysis

Both surface soil EC and SAR were strongly correlated with fall bands and indices compared to spring and summer (Table 2.3). Highest correlation was found with blue band (B2) for both EC ($r=0.79^{*}$) and SAR ($r=0.61^{*}$). Thermal bands (B10 and B11) were more important in spring season when ground was not covered by green vegetation. For DEM parameters elevation was strongly correlated with soil salinity and sodicity.

Time series analysis of Landsat 7 and Landsat 5 data

Time series data (1999-2015, Landsat 7 and 1999-2011, Landsat 5) were statistically analyzed for monotonic trend using Mann-Kendall test (Mann, 1945; Kendall, 1975; Hipel and McLeod, 1994). This test is non-parametric and does not require residuals to be normally distributed. This test assesses that if the variable is monotonically going upward (positive τ) or downward (negative τ) over the time period even though trend may or may not be linear. Mann-Kendall test on Landsat 7 time series (Table 2.4) showed statistically significant negative τ (-0.07) for short wave infrared (SWIR) bands (B5 and B7). This trend was observed on soil with higher EC (EC class >20 dS/m). Most probably these points are the EC hotspot where vegetation grows sparsely. Correlation analysis in Table 2.3 indicates that SWIR band (B6 and B7 of Landsat 8) are negatively correlated with EC and SAR during spring season. Hence, further decline on these bands as shown by Mann-Kendall test indicates that hot spot or salinity intensity increased from 1999 to 2015.

Mann-Kendall test on Landsat 5 time series (Table 2.5) showed that the NIR (B4) had a negative τ along with short wave infrared (SWIR) bands (B5 and B7). Response of NIR band was observed in all soil EC classes. Mann-Kendall test further allowed us to pick the most responsive bands for salinity assessment. Our study showed best band to monitor soil EC changes are SWIR and NIR even though several other bands showed strong linear correlations (Table 2.3). These results are in agreement with Shrestha (2006) and Bannari et al. (2008).

Table 2.3 Correlation between Landsat 8 TOA reflectance bands, indices and DEM parameters with surface soil EC and SAR at Pierpont

		Spring		Summer		Fall	
Band/index	Wavelength (μm)	EC	SAR	EC	SAR	EC	SAR
B1	0.43 - 0.45	0.35	0.30	0.60	0.54	0.75	0.61
B2	0.45 - 0.51	-0.02	0.04	0.61	0.51	0.79	0.61
B3	0.53 - 0.59	-0.32	-0.17	0.46	0.36	0.61	0.55
B4	0.64 - 0.67	-0.40	-0.33	0.39	0.36	0.66	0.50
B5	0.85 - 0.88	-0.42	-0.38	-0.46	-0.45	-0.64	-0.49
B6	1.57 - 1.65	-0.43	-0.42	0.49	0.43	0.62	0.50
B7	2.11 - 2.29	-0.26	-0.34	0.55	0.49	0.63	0.54
B9	1.36 - 1.38	0.49	0.29	0.05	0.03	-0.33	-0.15
B10	10.60 - 11.19	-0.49	-0.45	-0.07	0.00	-0.57	-0.44
B11	11.50-12.51	-0.50	-0.47	0.06	0.04	-0.41	-0.33
BI		-0.42	-0.37	-0.42	-0.41	-0.61	-0.46
NDVI		0.03	-0.05	-0.56	-0.54	-0.73	-0.55
NDSI		-0.03	0.05	0.56	0.54	0.73	0.55
NDMI		-0.11	-0.17	0.60	0.55	0.70	0.54
NDWI		-0.25	-0.38	-0.61	-0.56	-0.74	-0.60
SAVI		-0.18	-0.24	-0.56	-0.53	-0.70	-0.54
SI		-0.29	-0.22	0.48	0.43	0.74	0.56
MIRBI		0.65	0.45	0.18	0.20	0.51	0.51
Elevation		-0.51	-0.46	-	-	-	-
Slope		0.36	0.20	-	-	-	-
Aspect		0.11	0.14	-	-	-	-

Table 2. 4 Mann-Kendall test for monotonic trend (τ) of Landsat 7 time series (1999 – 2015) data. P-value are for two-sided test.

Band	Wavelength	EC <2 (n =81)		EC >20 (n=31)		EC 10-20 (12)	
	(μm)	τ	P value	τ	P value	τ	p-value
B1	0.45-0.52	-0.008	0.83	-0.017	0.67	-0.01	0.76
B2	0.52-0.60	-0.01	0.71	-0.023	0.55	-0.02	0.61
B3	0.63-0.69	-0.01	0.76	-0.029	0.47	-0.02	0.57
B4	0.77-0.90	-0.01	0.74	-0.018	0.68	-0.01	0.74
B5	1.55-1.75	-0.045	0.27	-0.075	0.07	-0.06	0.14
B6	10.40-12.50	0.02	0.53	0.032	0.42	0.03	0.46
B7	2.09-2.35	-0.03	0.37	-0.07	0.09	-0.055	0.18
B8	0.52-0.90	-0.03	0.46	-0.02	0.57	-0.018	0.66

Table 2.5 Mann-Kendall test for monotonic trend (τ) of Landsat 5 time series (1999 – 2011) data. P-value are for two-sided test.

Band	Wavelength	EC <2 (n =81)		EC >20 (n=31)		EC 10-20 (n=12)	
	(μm)	τ	P value	τ	P value	τ	p-value
B1	0.45-0.52	-0.06	0.38	-0.02	0.78	-0.03	0.61
B2	0.52-0.60	-0.05	0.42	-0.02	0.80	-0.03	0.61
B3	0.63-0.69	-0.07	0.32	-0.04	0.50	-0.05	0.47
B4	0.76-0.90	-0.15	0.02	-0.17	0.01	-0.16	0.02
B5	1.55-1.75	-0.007	0.91	-0.13	0.05	-0.10	0.13
B6	10.40-12.50	0.01	0.79	0.02	0.78	0.01	0.82
B7	2.08-2.35	0.02	0.75	-0.13	0.06	-0.10	0.14

Soil surface EC model comparison using 2013 and 2014 April image

Soil EC data was positively skewed to right with Pearson skewness coefficient of 2.01. Hence EC variable was log-transformed for further analysis in model building stage.

Semivariance of surface soil EC (Fig. 2.6) shows that they were spatially correlated up to 200 m. One of the criteria for model selection was to identify how much spatial autocorrelation was reduced by the model. For comparison, semivariogram range value was fixed to 100 m distance and the resulting sill values of different models were compared. For the beginning, models developed on April 17, 2014 image were compared. Inputs used were image bands, indices developed from those bands and DEM parameters. The reason to use single image was to remove other confounding factors and compare models and bands that appear important for salinity prediction.

Multiple linear regression was performed in stepwise method. Overall, all models (linear regression, LR; regression tree, RT; cubist; and random forest, RF) showed fairly high R^2 (>70%) value on training data set (Table 2.6). Random forest showed highest R^2 (0.77) on validation data set. Semivariance (sill value) of the model residuals shows that only random forest method was able to completely remove spatial correlation. Linear regression method was weakest in terms of modeling autocorrelation (sill value = 0.89).

Important variables selected by linear regression were, B6 (1.57 - 1.65 µm), B5 (0.85 - 0.88 µm), NDVI, and elevation. Random forest showed B6 (1.57 - 1.65 µm), B7 (2.11 - 2.29 µm), NDVI, B10 (10.60 - 11.19 µm), B11 (11.50-12.51 µm) and Elevation as major contributor on the model. To identify important Landsat 8 bands, random forest model was rerun with those bands only (DEM was removed). Rerun model showed SWIR bands B7, B6 and thermal band B11 and B10 were the important bands for the EC prediction (Fig 2.7). Important variables were determined by increase in mean square error (MSE) when these variables were removed from the fitted model. Short wave infrared (SWIR) band B6 and B7 appeared very important as their removal from fitted model increased MSE nearly 20%.

Random forest model was chosen for further analysis. Principle component (PC) of image bands (B1-7 and B10-11) of year 2013 and 2014 and DEM parameters (elevation, slope and aspect) were compared. Additional data set from Redfield was used as independent validation site. Results showed that model predictability was similar to the original bands. Predictability (R^2 value) within Pierpont site (both for training and validation data) were high but it decreased when tested in the independent test site, Redfield. Predictability was lower when previous crop was corn (2013, R^2= 0.25) compared to soybean (2014, R^2= 0.40) in the training site (Pierpont). This might be due to higher soil coverage by corn stover compared to soybean stubble. Combining two years (2013 and 2014) improved predictability at both validation (R^2= 0.82) and test (R^2= 0.50) site. Addition of DEM further increased soil EC predictability. Figure 2.8 and 2.9 shows the predicted map using this method for both Pierpont and Redfield site.

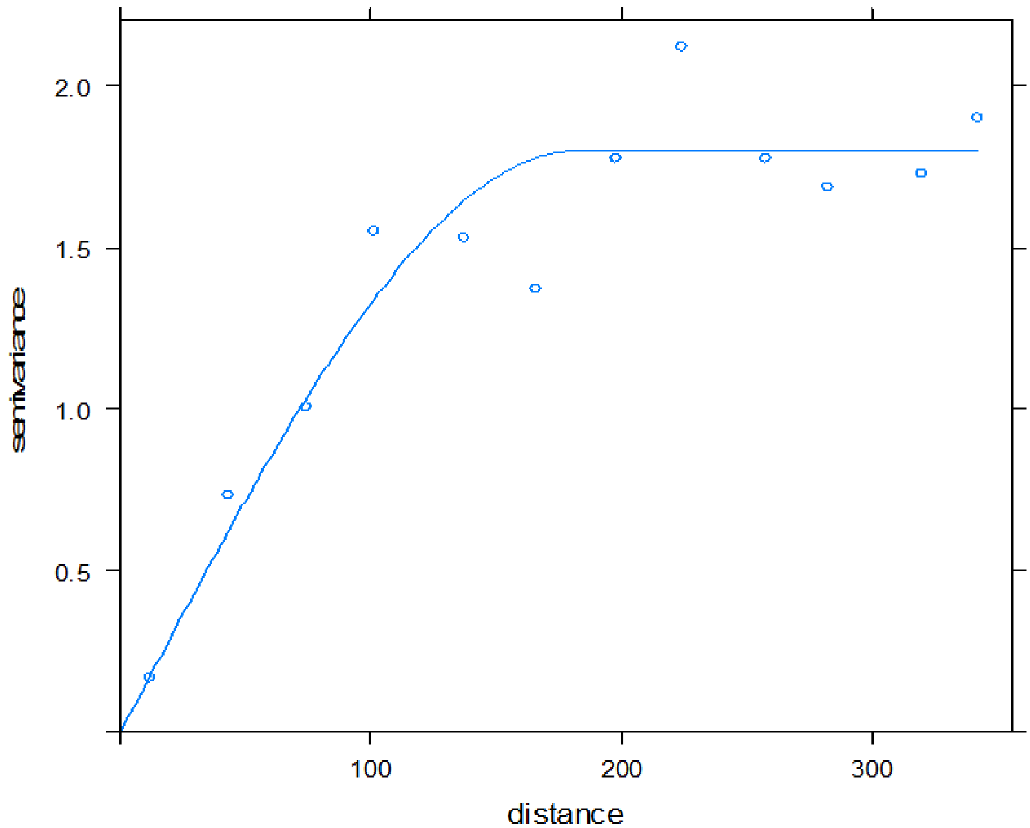

Figure 2.6 Semivariance of surface soil EC (0- to7.5- cm). EC data were natural log transformed.

Table 2.6 Model comparison for predicted soil surface EC using 2014 Landsat image. Data points were randomly divided between training (n=134) and validation (n=70) set for Pierpont site. Landsat image bands, DEM and reflectance indices were used for model building. Models compared were linear regression (LR), regression tree (RT), cubist and random forest (RF) methods.

Model	Training R^2	Validation R^2	RMSE	Bias	Range (m)	Sill value	nugget
LR*	0.76	0.65	0.028	-0.028	100	0.89	0.05
RT	0.75	0.68	0.79	-0.12	100	0.67	0.06
Cubist	0.79	0.71	0.75	-0.02	100	0.55	0.07
RF	0.70	0.77	0.68	-0.03	100	0.06	0.11

Note: * Multiple linear regression was performed with stepwise selection method. Variable to enter and stay were defined at p-value 0.2 and 0.05 respectively. Variable with high variance inflation ratio (VIF>15) were removed from the model.

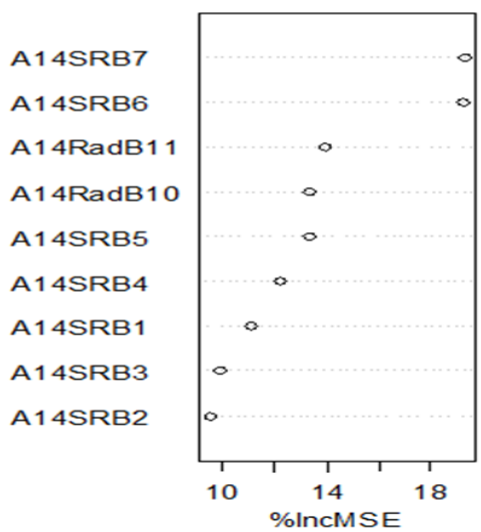

Figure 2. 7 Variable of Importance plot of Random Forest model for surface soil EC prediction. Variables with higher % increase in mean square error (MSE) are most important for the model. Variables are coded as A14SRB= April 2014 Surface Reflectance Band, and A14RadB= April 2014 Radiance Band.

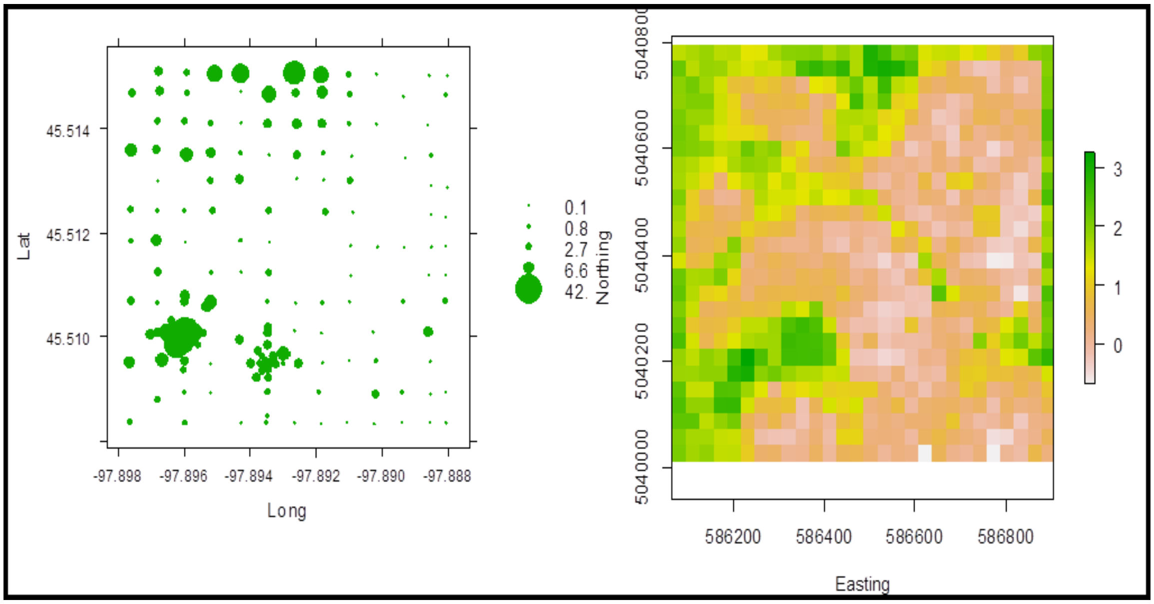

Figure 2.8 Observed soil EC in dS/m (left) and predicted log of EC (right) using Random Forest method for Pierpont site. Model used principle component of both 2013 and 2014 April image surface reflectance + DEM parameters (R^2= 0.78).

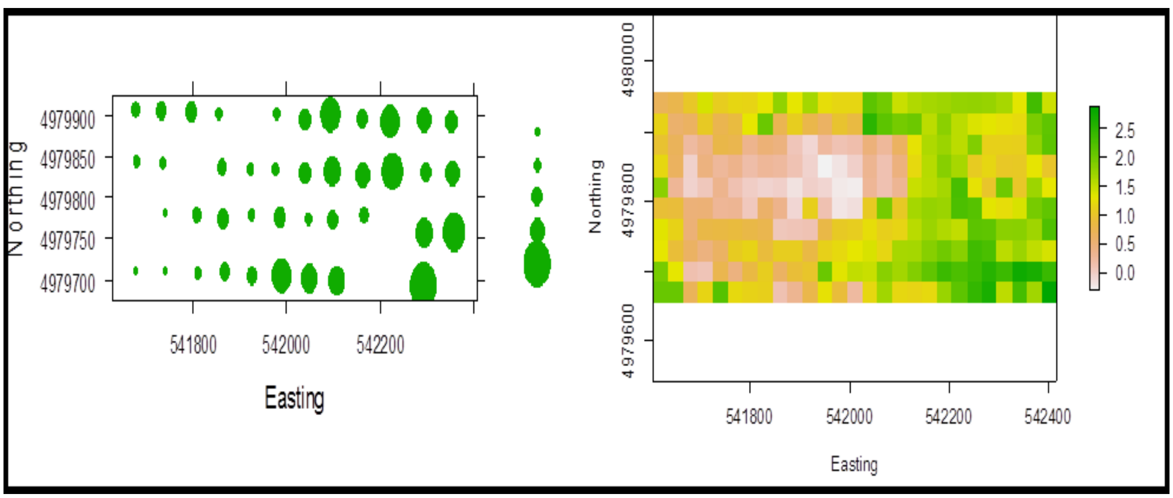

Figure 2.9 Redfield observed soil EC in dS/m(left) and predicted log of EC (right) using Random Forest model developed from Pierpont data. Model used principle component of both 2013 and 2014 April image surface reflectance + DEM parameters (R^2 =0.56).

Soil EC prediction for state of South Dakota

Random forest model as indicated best in previous stage was used to predict soil EC for state of South Dakota. Planetary scale mapping platform Google Earth Engine API was used for this purpose. Both sites (Pierpont and Redfield) were used as training data and separate 65 samples collected from eastern South Dakota as model validation data. In this stage, combination of all 3-season image (3 year median image such as 2011-2013 median spring, summer and fall images for EC year 2012) showed highest R^2 with state wide validation data set (R^2 = 0.26) and relationship was better with SSURGO database EC value (Table 2.8). EC map produced by this method (3-year median images) are shown in figures 2.10 and 2.11 and summary statistics of all 3-season model predicted EC in Table 2.7. These results indicate that combining all 3-season images improve EC prediction in regional scale. EC predicted using all 3-season image was used to detect change in acreages in eastern South Dakota.

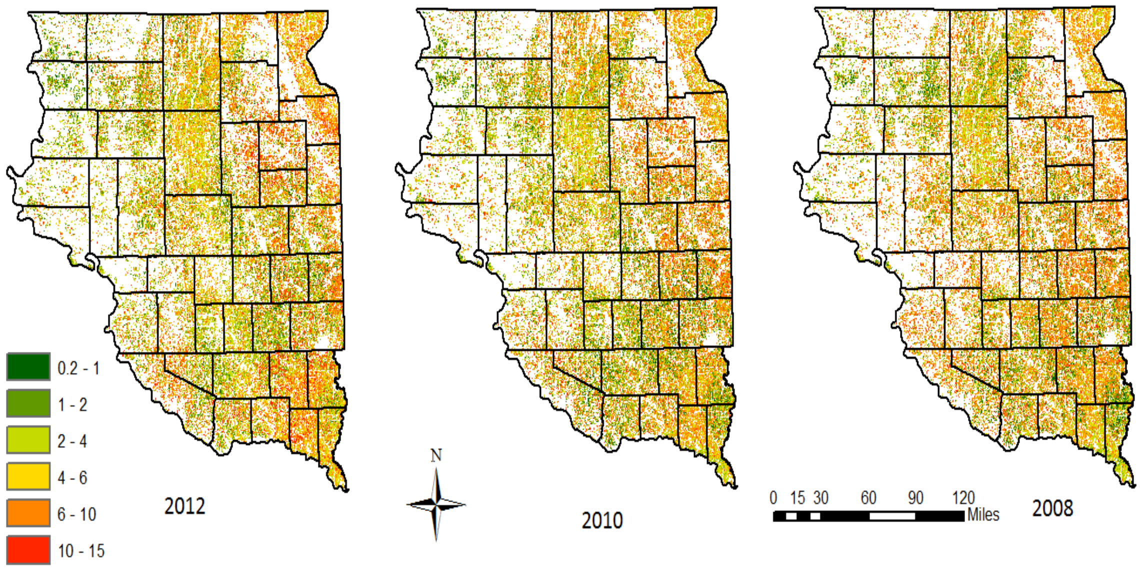

Figure 2.10 Predicted EC (dS/m) eastern South Dakota using spring season covariates.

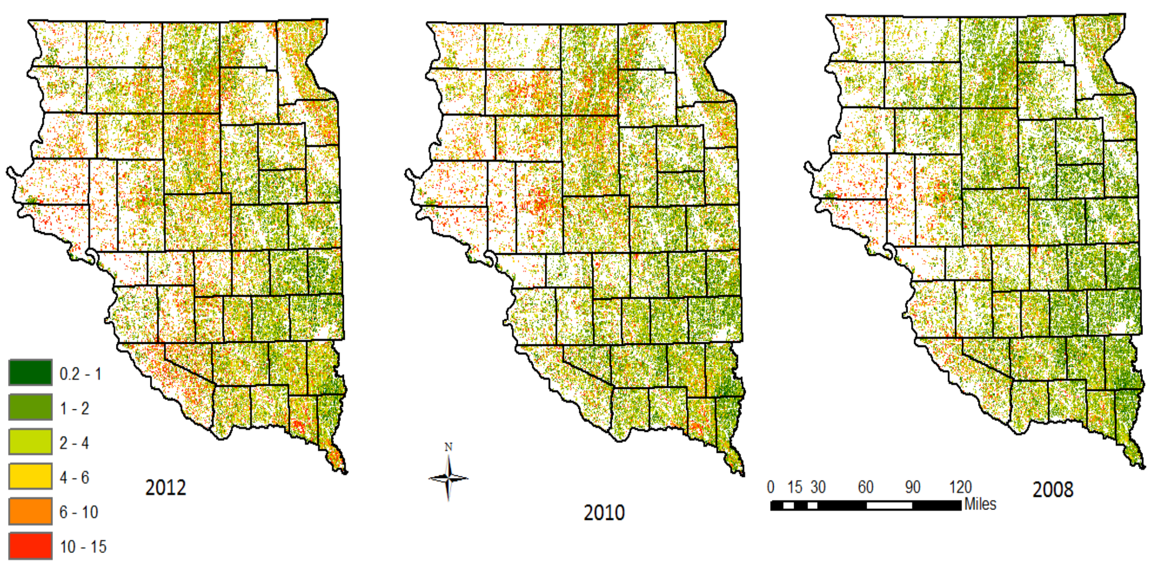

Figure 2.11 Predicted EC (dS/m) for eastern South Dakota using all 3 season covariates (Spring + Summer + Fall). Refer Table 2.8 for validation result.

Table 2.7 Summary of predicted electrical conductivity (dS/m) using 3-year Landsat image + elevation model for each of 6 land capability class (LCC) in eastern South Dakota cropland data points.

EC Year	LCC	Mean	Median	S.D.	Min	Max	N
2008	1	2.3	1.7	1.9	0.7	18.7	334
2008	2	3.0	2.0	2.8	0.5	22.3	2524
2008	3	2.8	1.9	2.4	0.5	15.5	422
2008	4	3.2	2.2	2.6	0.7	15.4	349
2008	5	3.2	1.8	3.8	1.0	15.1	25
2008	6	4.1	3.1	3.7	0.7	17.5	76
2010	1	2.3	1.9	1.6	0.6	13.8	334
2010	2	2.8	2.1	2.2	0.4	18.3	2524
2010	3	2.9	2.1	2.2	0.6	13.4	422
2010	4	3.6	2.4	3.0	0.6	16.5	349
2010	5	3.2	2.1	3.0	0.6	12.7	25
2010	6	4.4	3.0	3.7	0.8	15.4	76
2012	1	3.4	2.3	2.8	0.5	19.7	334
2012	2	4.2	2.8	3.4	0.3	23.1	2524
2012	3	4.1	3.1	3.2	0.4	17.6	422
2012	4	5.0	3.6	4.0	0.7	16.9	349
2012	5	4.3	2.8	3.6	1.3	14.7	25
2012	6	6.2	4.4	4.7	0.6	19.1	76

Table 2.8 Validation of the Random Forest model based on soil EC values from the SSURGO soil mapping units. This validation only included fields that were cropped with soybeans and corn.

LCC	N	SSURGO Database EC (dS/m)				Model EC and SSURGO EC relationship
		Mean-Rep*	S.D.	Mean-High*	S.D.	
1	334	1.10	0.88	2.16	1.50	2008EC = 0.9 x + 1.51,
2	2524	1.41	1.84	2.67	2.97	R^2 =0.63), (Pr =0.06)
3	422	1.43	2.23	2.70	3.82	2010EC = 1.1 x + 1.25,
4	349	2.01	2.59	3.62	4.02	R^2=0.62, (Pr= 0.06)
5	25	2.40	2.08	4.00	3.21	2012EC =1.3 x + 2.24,
6	76	2.24	2.83	4.00	4.46	R^2=0.50, (Pr=0.11)

*SSURGO table EC Representative (Mean-Rep) and EC High (Mean-High) value

EC change from 2008 to 2012 in eastern South Dakota

Soil EC predicted using all 3 season image (Table 2.7) ranged from 2.3 to 6.2 for LCC 1 to 6 over the year 2008 to 2012. Predicted soil EC closely matched with SSURGO database EC (Table 2.8). Predicted EC were always higher than SSURGO representative EC value. Measured soil EC at Pierpont and Redfield (245 sampling points, data not shown) showed similar higher value compared to SSURGO soil EC value. Aggregated over soil map unit, surface soil EC value we observed at Pierpont and Redfield site was 3.9 (±2.5) while SSURGO EC value for those points were 1.0 (±0.3). Coefficient of determination (R^2) between SSURGO database EC representative value and predicted EC was 0.63, 0.62 and 0.50 for EC year 2008, 2010 and 2012 respectively (Table 2.8). Strong relationship of predicted soil EC with SSURGO database indicates that multiyear Landsat image can be very useful to predict soil salinity at higher spatial resolution.

Soil EC was more affected by previous year's growing season precipitation than the current year precipitation for each EC-year (Table 2.9 and 2.10). EC increased with previous year's precipitation in 2008 (Table 2.10) while it decreased with current year precipitation in 2008 and 2012. Growing season maximum temperature always showed positive relationship with soil EC whereas minimum temperature showed no relationship at all during same period.

The result of such a trend can be implied that precipitation from previous year that contributes to water table rise and that eventually bring salt to the surface with increasing temperature (Eisenlohr and Sloan, 1968; Anderson et al., 2012). Spring rainfall has increased in the region (Clay et al., 2014). For example, precipitation increased from 41 to 63 cm since 1939 in Brookings South (Anderson et al., 2012). This rise in temperature and higher rainfall reduced the risk of growing annual crops in the region (Schrag, 2011; Clay et al., 2014; Cook et al., 2015; Reitsma et al., 2015). Reistma et al., 2015 reported 728,000 hectares of land were converted from grassland to croplands in South Dakota between 2006 and 2012 due to this favorable weather condition. However this conversion from grassland to cropland reduced transpiration, which further increased water table rise, salinization and sodicity.

EC predicted using all 3 season images (Table 2.11) shows that salinity in eastern South Dakota increased on 13.4% of the corn soybean acreages from year 2008 to 2012. This calculation is based on at least 4 dS/m increase in EC value. This threshold value (4 dS/m) was chosen considering the standard deviation of predicted EC (Table 2.7). Acreage with increased soil EC was lower (8.3%) with spring season image model compared to all 3-season image model. This is because spring season model predicted soil EC to be very high in each year (Fig 2.10) and the predicted values were always high compared to SSURGO soil EC value. Hence more reliable estimation appears to be model developed using all 3-season image for the region (Fig. 2.11).

EC change per LCC was evaluated using eastern South Dakota land-use change dataset (Table 2.12). Most of the data points were in LCC 2 and we observed 12.7 % of those data points showed increase in soil EC from year 2008 to 2012.

Table 2.9 Weather Data for each of the Land capability class during model estimation period. Growing season is April 1 to September 30. For each EC year, weather data are shown for previous year (Year Before) and same year growing season.

	LCC	Growing Season Precipitation (mm)		Growing Season Tmax (K)		Growing Season Tmin (K)	
EC Year		Year Before	Same Year	Year Before	Same Year	Year Before	Same Year
2008	1	466.0	460.0	297.3	296.0	284.7	283.1
2008	2	490.4	439.8	297.4	296.3	284.4	282.7
2008	3	499.6	445.4	297.0	296.0	284.2	282.6
2008	4	503.0	446.7	297.6	296.5	284.6	282.9
2008	5	474.1	462.6	297.5	296.3	284.7	283.1
2008	6	500.5	442.8	297.6	296.5	284.5	282.8
2010	1	435.6	755.4	295.4	297.0	282.9	284.6
2010	2	411.9	641.3	295.6	297.0	282.6	284.3
2010	3	413.7	623.4	295.3	296.7	282.5	284.2
2010	4	431.0	669.7	295.8	297.2	282.8	284.5
2010	5	445.6	741.8	295.6	297.1	282.9	284.6
2010	6	415.6	690.7	295.8	297.2	282.7	284.4
2012	1	468.6	342.2	298.2	300.9	283.9	285.1
2012	2	452.0	318.6	298.2	300.9	283.6	284.9
2012	3	455.6	329.2	297.9	300.4	283.4	284.7
2012	4	455.5	318.2	298.5	301.1	283.8	285.0
2012	5	493.1	340.6	298.3	301.1	283.9	285.2
2012	6	464.5	318.4	298.5	301.2	283.7	285.0

Table 2.10 Relationship between weather data and predicted soil EC. For each EC year linear relationship between weather data are shown for previous year (Year Before) and same year growing season.

EC Year	Variable	Linear Relationship	
		Year Before	Same Year
2008	Precip.(mm)	0.03x - 8.1, R^2=0.37	-0.03x +16.0, R^2=0.22
2008	Tmax (ºK)	1.58x -468, R^2= 0.38	2.12x - 625, R2= 0.66
2010	Precip.(mm)	No linear relationship	No linear relationship
2010	Tmax (ºK)	2.83x -833, R^2= 0.65	2.4x -707, R^2= 0.38
2012	Precip.(mm)	No linear relation	-0.06x +24.50, R^2 =0.47
2012	Tmax (ºK)	2.91x- 866, R^2=0.46	1.8x -537, R^2 =0.28

Table 2.11 Acres and percentage affected by at least 1 standard deviation (4 dS/m , based on Table 2.7) EC increase in eastern South Dakota corn + soybean field pixels.

EC model	2008-2010		2010-2012		2008-2012	
	hectares	%	hectares	%	acres	%
All 3 Season	106540	2.5	462991	10.9	569165	13.4
Spring Season	201329	4.8	315083	7.4	349931	8.3

Total Corn + Soy area in 2014 for eastern South Dakota was 4237065 ha. Percentages are Calculated based on Corn + Soybean pixels in crop data layer (CDL) 2014.

Table 2.12 Percentage change in sol EC for each of LCC based on 3730 eastern South Dakota cropland data points. Points with >1 SD increase in soil soil EC was used to calculate these percentage.

LCC	Total Observation	>1 SD increase	Change	2008 EC (dS/m)		2012 EC (dS/m)	
	# of points	# of Points	%	Mean	Median	Mean	Median
1	334	35	10.5	2.3	1.7	3.4	2.3
2	2524	321	12.7	3.0	2.0	4.2	2.8
3	422	56	13.3	2.8	1.9	4.1	3.1
4	349	62	17.8	3.2	2.2	5.0	3.6
5	25	2	8.0	3.2	1.8	4.3	2.8
6	76	16	21.1	4.1	3.1	6.2	4.4

Conclusions

This paper tests series of hypotheses starting from how ground based and remotely sensed reflectance respond to soil salinity to what machine learning techniques effectively utilize that reflectance to map soil salinity. Our result shows that within agricultural fields in NGP, soil reflectance decreases with both soil EC and SAR. Random forest method was the most effective machine learning techniques to map soil salinity because of its ability to capture spatially correlated variation. In addition, this paper explored what bands can be used to monitor soil salinity changes in long run and results show that SWIR bands (B5 and B7 in Landsat 7 and Landsat 5, and B6 and B7 in Landsat 8) and NIR (B4 in Landsat 5) were more sensitive to increasing soil salinity. Finally soil EC was predicted for eastern South Dakota using spring, summer, fall and all 3-season combined images. Predicted soil EC was influenced by crop type and the residue cover. Results show that spring image was best input for EC prediction using random forest model for a specific field but all 3-season image combined was better for regional level estimation. Estimated acres with increased soil EC in eastern South Dakota from 2008 to 2012 was 569,165 ha or 13.4 % of soybean and corn acreages in this region.

References

Anderson, J.P., B.O. Kunze, N. A. Andersen, and S.R. Burchkart. 2012. Precipitation and Water Table Measurement Comparison Study for 2010 and 2011 for Brookings, South Dakota COOP (Co-operative Observer Program) Weather Station and AWDN (Automated Weather Data Network) Weather Station and a Look At How 2010 Was a Record Breaking Precipitation Year. American Meteorological Society. https://ams.confex.com/ams/92Annual/webprogram/Paper202238.html

Bannari, A., A. M. Guedon, A. El-Harti, F.Z. Cherkaoui, and A. El-Ghmari. 2008. Characterization of slightly and moderately saline and sodic soils in irrigated agricultural land using simulated data of Advanced Land Imaging (EO-1) sensor. Commun. Soil Sci. Plant Anal. 39:2795–2811

Breiman, L., J. Friedman, R. Olshen, and C. Stone. 1984. Classification and Regression Trees. Wadsworth, Pacific Grove, CA.

Carlson, C.G., D.E. Clay, K. Reistma, and R. Gelderman. 2013, Soybeans, salinity, and sodicity. Chapter 48. *In* Clay, D.E., C.G. Carlson, S.A. Clay, L. Wagner, D. Deneke, and C. Hay. (eds). iGrow Soybean: Best Management Practices. South Dakota State University

Chang, J., S. A. Clay, D. E. Clay, and K. Dalsted. 2004. Detecting weed-free and weed-infested areas of a soybean field using near-infrared spectral data. Weed Science. 52: 642-648.

Chander, G., B.L. Markham, and D. L. Helder. 2009. Summary of current radiometric calibration coefficients for Landsat MSS, TM, ETM+, and EO-1 ALI sensors. Remote Sens. Environ. 113:893-903.

Clay, D., S. Clay, K. Reitsma, B. Dunn, A. Smart, G. Carlson, D. Horvath, and J. Stone. 2014. Does the conversion of grasslands to row crop production in semi-arid areas threaten global food security? Global Food Security. 3:22-30. Available at http://www.sciencedirect.com/science/journal/22119124/3

Cook, B. I., T. R. Ault, and J. E. Smerdon. 2015. Unprecedented 21st century drought risk in the American Southwest and Central Plains. Sci. Adv. 1(1):e1400082. doi: 10.1126/sciadv.1400082.

Eisenlohr, W.D., and C.E. Sloan. 1968. Generalized hydrology of prairie potholes on the Coteau de Missouri, North Dakota. USGS Circular 558, available at http://pubs.usgs.gov/circ/1968/0558/report.pdf

Google Earth Engine Team. 2015. Google Earth Engine: A planetary-scale geo-spatial analysis platform [WWWDocument]. http://earthengine.google.com

Hadrich, J. 2012. Managing the economics of soil salinity in the Red River Valley of North Dakota. J American Society of Farm Managers and Rural Appraisers. p. 80-88. http://purl.umn.edu/190726

He, Y., T.M. DeSutter, F.X.M. Casey, L.J. Cihacek, D.E. Clay, D. Franzen, and D.D. Steele. 2014. Behaviors of Na-affected soil and implications for subsurface drainage. American Society of Agronomy meeting, Nov 2-5, 2014, Long Beach CA.

He, Y., T.M. DeSutter, and D.E. Clay. 2015a. The relationship between SAR1:5 and SARe of three extraction methods. Soil Sci. Soc. Am. J. 79:681-687.

He, Y., T. DeSutter, D. Franzen, D. Steele, and D.E. Clay. 2015b. Field capacity water as influenced by Na and EC: Implications for subsurface drainage. Geoderma. 245-246:83-88.

Hipel, K.W. and A. L. McLeod. 1994. Time Series Modelling of Water Resources and Environmental Systems. Elsevier, Amsterdam.

Hopkins, D., K. Chambers, A. Fraase, Y. He, K. Larson, L. Malum, L. Sande, J. Schulte, E. Sebesta, D. Strong, E. Viall, and R. Utter. 2012. Evaluating salinity and sodium levels on soils prior to drain tile installation: a case study. Soil Horizons 53:24-29.

Howari, F.M. 2003. The use of remote sensing data to extract information from agricultural land with emphasis on soil salinity. Soil Research. 41: 1243-1253. doi:http://dx.doi.org/10.1071/SR03033.

Howari, F.M., P.C. Goodell, and S. Miyamoto. 2002. Spectral properties of soil crusts on saline soils. J. Environ. Qual. 31:1453-1461.

Jenny, H. 1941. Factors of soil formation. McGraw-Hill, New York, NY.

Joshi, D. C., T. Toth, and D. Sari. 2002. Spectral Reflectance Characteristics of Na-carbonate Irrigated Arid Secondary Sodic Soils. Arid Land Research and Management. 16 (2): 161-176, DOI: 10.1080/153249802317304459.

Kendall, M.G. 1975. Rank Correlation Methods, 4th edition. Charles Griffin, London.

Lobell D.B., D. Thau, C. Seifert, E. Engle, B. Little. 2015. A scalable satellite-based crop yield mapper. Remote Sens. Environ. 164:324-333. DOI: 10.1016/j.rse.2015.04.021.

Lobell, D.B., S.M. Lesch, D.L. Corwin, M.G. Ulmer, K.A. Anderson, D.J. Potts, et al. 2010. Regional-scale assessment of soil salinity in the Red River Valley using multi-year MODIS EVI and NDVI. J. Environ. Qual. 39: 35-41. doi:10.2134/jeq2009.0140.

Mann, H.B. 1945. Non-parametric tests against trend. Econometrica 13:163-171.

Masoud, A. A., and K. Koike. 2006. Constructing a Groundwater Potential Model for an Arid Environment Integrating Remote Sensing and GIS. Memoirs of the Faculty of Engineering, Kumamoto University. 50: 53-68.

McBratney, A. B., M. L. Mendonça Santos, and B. Minasny. 2003. On digital soil mapping. Geoderma 117: 3-52.

McIntyre, D. S. 1979. Exchangeable sodium , subplasticity and hydraulic conductivity of some Australian soils. Aust. J. Soil Res. 17:115-120.

Metternicht, G.I., and J. A. Zinck. 2003. Remote sensing of soil salinity: Potentials and constraints. Remote Sens. Environ. 85: 1–20.

Millar, J. 2003. Managing Salt affected soil. SD Notill Newsletter.Available: http://www.sdnotill.com/Newsletters/2003_Salt_Soils.pdf

National Soil Survey Center. 1996. Soil Survey Methods Laboratory Manual, USDA-NRCS.

Nawar, S., H. Buddenbaum, J. Hill, J. Kozak. 2014. Modeling and mapping of soil salinity with reflectance spectroscopy and Landsat data using two quantitative methods (PLSR and MARS). Remote Sens. 6:10813-10834.

Northcote, K.H., and J. K. M. Skene. 1972. Australian soils with saline and sodic properties. Soil Publ. 27. CSIRO Publ. Melbourne, Australia

NRCS. 2012. Economic impact of saline soils in Upper James River. SD-FS-81.available at http://www.nrcs.usda.gov/Internet/FSE_DOCUMENTS/nrcs141p2_035584.pdf

Pachepsky, Y. A., D. J. Timlin, and W. J. Rawls. 2001. Soil water retention as related to topographic variables. Soil Sci. Soc. Am. J. 65: 1787-1795.

Rao, B. R. M., R. C. Sharma, T. Ravi Sankar, S. N. Das, R. S. Dwivedi, S. S. Thammappa and L. Venkataratnam. 1995. Spectral behaviour of salt-affected soils. Int. J. of Rem. Sens. 16: 2125-2136.

Reitsma, K.D., B.H. Dunn, U. Mishra, S. A. Clay, T. DeSutter, and D. E. Clay. 2015. Land-use change impact on soil sustainability in a climate and vegetation transition zone. Agron. J. 107: 2363-2372.

Rhoades, J. D., and A. D. Halverson. 1976. Detecting and delineating saline seeps with soil resistance measurements. Regional Saline Seep Control Symposium Proceedings, Montana State University, Cooperative Extension Service Bul. 1132, 19-34.

Schrag, A.M. 2011. Addendum: climate change impacts and adaptation strategies. *In* Forrest, S.C., H. Stand, W.H. Haskins, C. Freese, J. Proctor, and E. Dinerstein (eds.). Ocean of grass: A Conservation Assessment for the Northern Plains Conservation Network and Northern Great Plains Ecoregion. World Wildlife Fund-US, Bozeman MT, Available at http://kresge.org/sites/default/files/Uploaded%20Docs/WWF%20-%20Ocean_Grass.p

Schmid, T., M. Koch, and J. Gumuzzio. 2009. Applications of hyper-spectral imagery to soil salinity mapping. pp 113-140. *In*: Remote Sensing of Soil Salinization: Impact on Land Management; Metternicht, G., Zinck, J., Eds.; CRC Press: Boca Raton, FL, USA.

Seelig, B. D. 2000. Salinity and sodicity in North Dakota soils. NDSU Extension. http://www.ndsu.edu/soilhealth/wp-content/uploads/2013/03/ND-saline-sodic-soils_2000.pdf.

Shatar, T. M., and A. B. McBratney. 1999. Empirical modeling of relationships between sorghum yield and soil properties. Precision Agric. 1: 249-276.

Shrestha, R.P. 2006. Relating soil electrical conductivity to remote sensing and other soil properties for assessing soil salinity in northeast Thailand. Land Degrad. Dev.17: 677–689.

Sidike, A., S. Zhao, and Y.Wen. 2014. Estimating soil salinity in Pingluo county of China using QuickBird data and soil reflectance spectra. Int. J. Appl. Earth Obs. Geoinf. 26:156–175.

Steinberg, D., and P. Colla. 1995. CART: tree-structured non-parametric data analysis. Salford Systems, San Diego, CA.

Suarez, D.L., J.D. Wood, and S.M. Lesch. 2008. Infiltration into cropped soils: Effect of rain and sodium adsorption ratio-impact irrigation water. J. Environ. Qual. 37(5):169-179.

Sumner, M. E., P. Rengasamy, and R. Naidu. 1998. Sodic Soils: A Reappraisal. In: Sodic Soils: Distribution, Properties, Management and Environmental Consequences. Eds. M. E. Sumner, R. Naidu. Oxford University Press. Oxford, New York.

Webster, R. and M. A. Oliver. 2001. Geostatistics for Environmental Scientist. Chichester: John Wiley and Sons. Pp 271.